CONF-790808--13

A COMPARISON OF NUMERICAL RESULTS WITH EXPERIMENTAL DATA FOR SINGLE-PHASE NATURAL CONVECTION IN AN EXPERIMENTAL SODIUM LOOP*

R. J. Ribando
Associate Member ASME

Oak Ridge National Laboratory
Oak Ridge, Tennessee 37830

MASTER

Submitted for presentation at the Technical Session on Transient Decay Heat Removal from Nuclear Reactors at the 18th National Heat Transfer Conference to be held in August 1979, San Diego, California.

---

*Research sponsored by the Division of Reactor Research and Technology, U.S. Department of Energy under contract W-7405-eng-26 with the Union Carbide Corporation.

ABSTRACT

A comparison is made between computed results and experimental data for single-phase natural convection in an experimental sodium loop. The tests were conducted in the Thermal-Hydraulic Out-of-Reactor Safety (THORS) Facility, an engineering-scale high temperature sodium facility at the Oak Ridge National Laboratory used for thermal-hydraulic testing of simulated LMFBR subassemblies at normal and off-normal operating conditions. Heat generation in the 19 pin assembly during these tests was typical of decay heat levels. Tests were conducted both with zero initial forced flow and with a small initial forced flow. The bypass line was closed in most tests, but open in one. The computer code used to analyze these tests [LONAC (LOw flow and NAtural Convection)] is an ORNL-developed, fast running, one-dimensional, single-phase finite difference model for simulating forced and free convection transients in the THORS loop. In addition to simulating specific experimental tests, the code has been used to predict results for some other conditions as well, including higher heat generation rates, less heat transfer through the test section walls, etc.

Comparison of LONAC results with experimental data shows fairly good agreement early in the transient, but shows the need for better thermal models of the heat dump and other loop components if long transients are to be simulated. While the THORS loop is only mildly prototypic of an LMFBR primary loop, this work has provided useful insights in the program for establishing natural convection as a viable means of removing decay heat in the event of loss of forced flow in a loop-type LMFBR.

INTRODUCTION

At full-power conditions buoyancy is of little importance to the operation of Liquid Metal Fast Breeder Reactors (LMFBRs). At shutdown conditions, however, buoyancy will increase the flow over what would be produced by pony motor operation alone. In fact, in current designs buoyancy-driven flow should cool a shutdown reactor enough to give a sufficient margin of safety in the unlikely event of a complete loss of forced flow. A state-of-the-art review of work in the area of natural convection in loop type LMFBRs in general and in the Fast Flux Test Facility (FFTF) in particular has been given by Additon and Parziale [1]. Singer et al. [2] have made an analogous review for pool-type LMFBRs.

Since no loop type reactors are presently operating in the U.S. (although the FFTF is scheduled for criticality in 1979), most work is aimed at analytically and experimentally verifying numerical models used in system codes such as DEMO[3] for predicting plant operation when making the transition to and operating in the natural convection mode[4]. The tests discussed and analyzed in this paper were conducted in the Thermal-Hydraulic Out-of-Reactor Safety (THORS) Facility, an engineering-scale high temperature sodium facility at the Oak Ridge National Laboratory (ORNL) used for thermal-hydrualic testing of simulated LMFBR subassemblies at normal and off-normal operating conditions. While not considered a valid surrogate for a reactor primary loop, a comparison of data obtained in THORS has been made with results obtained using LONAC (LOw flow and NAtural Convection)[5], an ORNL-developed one-dimensional, system-type, single-phase, finite difference numerical model for simulating THORS operation. The exercise has given valuable insight in the program for establishing natural convection as a viable means of removing decay heat in the event of loss of forced flow in a loop-type LMFBR.

Construction of the THORS Facility was completed in 1970 and the bundle used for the tests described in this paper is the sixth to be tested in the loop. Prior operation of the loop includes nearly 20,000 hours of isothermal operation and about 2000 hours with bundle power on. Prior operation includes studies of both unblocked (e.g. Ref. 6) and deliberately blocked (e.g. Ref. 7) simulated subassemblies.

Procedure

A. Test Facility

All tests discussed in this paper were conducted in the Thermal-Hydraulic Out-of-Reactor Safety [THORS -- formerly the Fuel Failure Mockup (FFM)] Facility, an isometric drawing of which is given in Fig. 1. Note that the pipe run containing the old test section was valved off during this test series. Forced flow is provided by a DC-motor-driven vertical-shaft centrifugal pump capable of delivering 40 ℓ/s at a pressure difference of 960 kPa. The loop piping can operate continuously at 700 kPa, and the loop components immediately downstream of the simulated LMFBR subassembly can withstand temperatures as high as 900°C for short time durations. Heat generation in the simulated LMFBR subassemblies is provided by electrically heated fuel pin simulator (FPS) units. Electrical capability has recently been expanded to 2 MW, however, heat dissipation capability is presently limited by the 0.5 MW heat dump. A 2 MW heat dump has been installed and will be connected to the loop piping when necessary. Pressure transmitters, flowmeters and thermocouples are installed to measure the system operating parameters. Electrical trace heaters are installed on all system lines to preheat the system and minimize heat losses during operation.

The power to the test section is provided by a three-phase grounded-wye ac electrical system. The FPSs are connected to each of the three electrical phases so that only the unbalanced current in the three-phase circuit returns through the neutral lead. Power is regulated by six controllers that activate zero-voltage-firing silicon-controlled rectifiers (SCRs) in series with the FPSs. Normally, each of five controllers feeds three FPSs and one controller feeds four heaters. The six separate control circuits can also be connected so that all FPSs may be operated from a common controller. Voltage to the FPSs may be varied by adjustable transformer taps on the supply transformers. The power to each set of FPSs can be controlled from 0 to approximately 51 kW per FPS.

A test-section inlet valve is available for simulating the pressure drop of the reactor inlet flow paths but was kept fully open in this test phase. A bypass line with a control valve which can be adjusted to give hydrodynamic simulation of other assemblies in a reactor core is in parallel with the test section. The hot sodium from the test section and sodium from the bypass line mix in the expansion tank. The expansion tank and the piping to it were designed to simulate the hydraulic characteristics downstream of a reactor core, and the expansion tank serves to mix hot and cold sodium, thus protecting the remainder of the loop from excessive temperatures. The ratio of bypass cross-sectional area to that in the test section is approximately 13:1. Programmable power control and programmable pump-speed control capabilities are provided so that prescribed and reproducible flow and/or power transients can be performed.

The pressure of the cover gas above the free surface in the pump bowl is normally regulated at a fixed level. That above the free surface in the expansion tank may be either fixed at the same level (by opening the cover gas equalizing valve HV-256) or allowed to float (HV-256 closed).

B. Bundle Description

The test section (referred to as Bundle 6A in this discussion) is a full-length simulated LMFBR fuel subassembly. It consists of 19 electrically-heated pins of 5.84 mm diameter spaced by 1.42 mm diameter helical wire-wrap spacers on a 305. mm helical pitch. The gap between the bundle and its containing hexcan is 0.71 mm, one-half the nominal pin-to-pin spacing. This configuration is used to flatten the sodium temperature across the bundle. In order to give a better simulation of the central region of a full reactor subassembly, appreciable effort was expended in designing and fabricating a low thermal inertia bundle housing. The bundle hexcan is 0.51 mm thick type 316 stainless steel backed by approximately 20 mm of calcium silicate block insulation contained in a stainless steel jacket [Fig. 2]. Early tests, however, indicated higher values for hexcan thermal inertia than expected and post-test examination revealed that sodium had indeed permeated the entire region. The impact of this sodium leakage on the tests will be discussed later.

The heated length of Bundle 6A is 0.9 m with variable-pitch heater windings to produce a 1.3 axial peak-to-mean chopped-cosine power distribution. Voltage is applied to each heating element through the copper lead at one end of the FPS, and the electric circuit is completed at the opposite end where the element is grounded through the end plug to the sodium. Each FPS is rated at 40 kW. The core inside the winding and the insulation between the winding and the type 316 stainless steel sheath is of compacted boron nitride [Fig. 3]. Downstream of the heated length, a nickel reflector and a simulated fission gas plenum have the same length and thermal inertia as an FFTF fuel assembly. Axial dimensions of the bundle are shown in Fig. 4.

Both the heated length and the simulated fission gas plenum are instrumented with wire-wrap thermocouples and duct-wall thermocouples. In addition, the heated length is instrumented with heater-internal thermocouples. The installation of heater internal and wire-wrap thermocouples is indicated in Fig. 3. Duct wall thermocouples are inserted into holes bored to within 0.121-0.25 mm of the inside surface of the hexcan. At the time of the tests discussed here, there were approximately 45 duct-wall, 33 wire-wrap and 43 heater internal thermocouples operating reliably in the bundle. Approximately 27 additional thermocouples were strapped to loop piping.

C. Data Acquisition

Data are recorded using a fast response Data Acquisition System (DAS) controlled by a PDP-8E computer. Data are stored on magnetic tape for subsequent processing and display. The procedure used for these tests is the fast scan mode in which data from 197 channels in a prescribed sequence are sequentially logged onto magnetic tape at 10,000 points per second for up to 12 minutes duration. Because of the extended duration of these tests, the fast scan mode was employed for periods of from 5 seconds to 5 minutes at up to approximately 25 times during the transients. In most cases a 5 minute scan was taken at the beginning of the test and then shorter (5 - 30 sec) scans were made at prescribed intervals. Subsquent changes to the DAS will allow continuous data recording at a slower scan rate for any future long-duration transients.

D. Test Procedure

One preliminary test and seven natural convection runs were run in this phase of the Bundle 6A test series. Earlier single-phase steady-state forced flow tests are reported in Ref. 8; later transient boiling tests are reported in Ref. 9. Because each of the tests involved a somewhat different procedure or different parameters, a table has been prepared listing parameters of each of the seven tests [Appendix I] and in this section narratives of these and the one preliminary test are given.

Test 32

The preliminary test involved determining trace heater settings around the loop (including pipe runs) for minimizing heat losses in the range of temperatures of interest. With the loop drained of sodium, individual trace heater circuits (there are some 36 on the main lines and components of the loop) were adjusted to maintain the specified temperature ±28°C as recorded by nearby loop thermocouples. This procedure was followed for temperatures of 316, 371, 427, 482, and 538°C. All loop temperatures and trace heater powers were recorded. Loop thermocouples and trace heater elements are strapped to the outside of the stainless steel piping, inside the Kaowool* insulation. Assuming that with sodium flowing inside the pipe most resistance to radial heat loss comes from the Kaowool insulation, then loop losses will be minimized if the sodium temperature is close to the specified temperature and the trace heat is set at the corresponding level. For instance, if the pipe trace heat is set at the level determined in the 427°C empty pipe test, then if the sodium temperature is about 427°C there will be no losses. If the sodium temperature is higher than 427°C,

*Babcock & Wilcox Company trade name.

there will be some loss from the sodium to ambient. If it is less than 427°C, some of the trace heat will actually flow into the sodium. Test 32 data can be found in Ref. 10.

Test 35

The objective of the first test was to determine the rate at which loop natural convection establishes from an initial specified low flow with a given bundle power. Hot leg trace heaters were at their 482°C settings, cold leg settings were at 316°C. As in all loop convection tests, trace heaters on the heat dump tubes and supplementary radiator heaters were off, the radiator damper was closed and the blower was off. With the bypass valve closed (as it was for all but Test 39) and the test section valve full open (as it was for all tests) a flow of about 0.13 ℓ/s (2.0 gpm) was established in the loop. Power to the bundle was turned on (9.0 kW total power) and approximately one half hour later, the pump was stopped to begin the test. About two and a half hours later the test was terminated.

Test 36

The purpose of Test 36 was to determine the rate at which loop natural convection develops from zero flow with a given uniform bundle power. Trace heater power was again based on 482°C in the hot leg piping and 316°C in the cold leg. The pump was stopped (a small flow will still persist because of temperature gradients in the loop). Approximately one half hour later the test was begun by energizing the bundle to 9.0 kW. The test was terminated after approximately one and one half hours.

Test 36A

This test was similar to Test 36 except that the equalizing gas valve (HV-265) between the expansion tank and the pump gas space was opened several

minutes after the pump was stopped. With this valve open there can be no pressurization of the argon cover gas in the expansion tank. Thus, the only driving forces are due to buoyancy and the elevation differences between the free surfaces in the pump bowl and the expansion tank. In addition the analysis is simplified because of not having to compute the cover gas pressure in the expansion tank. (Future tests will have instrumentation to measure cover gas temperature and pressure.) Data from this test indicate that the trace heater immediately upstream of the heat exchanger was not functioning during the test. It was repaired prior to the next test.

Test 36B

Test 36B, the test most extensively analyzed later in this paper, was similar to Test 36A. The only difference was that the trace heater settings for 316°C were used around the entire loop. All other tests used 482°C hot leg settings.

Test 37

The objective of Test 37 was to determine the effect of a steep power gradient on natural convection from an initial low flow. The test procedure was similar to that of Test 35 except that the heater power was as follows:

Pin No.	Nominal Heater Power (kW/rod)
8,9,10	0.9
2,3,11,19	0.7
1,4,7,12,18	0.5
5,6,13,17	0.3
14,15,16	0.1

Test 38

Test 38 used the same power skew as Test 37, but was initiated from zero flow. The procedure was identical to that of Test 37.

Test 39

This test was the only one in which the bypass was open to simulate a parallel bundle. With the hot leg trace heaters at the 482°C settings, the cold leg at the 316°C settings, the bypass line valve was adjusted to give about 0.13 ℓ/s (2 gpm) flow in the bypass line with 0.13 ℓ/s (2 gpm) in the test section. As in all cases the test section valve was full open. The trace heat in the bypass leg was raised to 7.3 kW total. Once temperatures had stabilized, the pump was stopped and the cover gas equalization valve (HV-265) was opened to begin the test. Approximately two hours later the test was concluded.

EXPERIMENTAL RESULTS

Of the seven tests run, three have been selected for discussion and analysis. These include one started from rest (Test 36B), one started from a low forced flow (Test 35) and the one test in which the bypass was open (Test 39). No analytical work has been done on Test 37 and Test 38 (which were run with an 80% power skew) since LONAC is one dimensional. Plots have been made of the temperature trace in the test section (e.g. Fig. 5A) during the early part of the transient and of the temperature trace around the loop at various times during the whole transient (e.g. Fig. 5B). The abscissa in both types of plots is distance along the loop in meters measured from the start of the heated section. Data in the test section are from wire-wrap (WW) or heater-internal (HI) thermocouples near the center of the bundle (i.e., thermocouples on pins 1-7). No WW or HI thermocouples were installed upstream of 0.53 m. Data from the rest of the loop are from thermocouples strapped to the outside of loop piping except for two thermocouples which are in wells inserted into the pipes at the test section inlet and outlet. Data from flowmeters will not be presented because of strong reservations over their validity at such low flows. Experimental heat balances using the indicated flow, temperature increase across the test section, and the bundle power were made throughout the transients. Those made toward the end of the runs, when transient heat storage effects in the bundle should be at a minimum, suggest flow meters generally reading some 50 - 80% high.

Test 36B has been selected for the most detailed analysis because with the cover gas equalization valve open, there is no cover gas pressurization to compute. The flow was at a virtual standstill when the bundle heat was switched on. Temperature fields in the bundle and in the whole loop are shown in Figs.

5A and 5B. Figure 5A indicates a temperature profile which is virtually symmetric with respect to the midpoint of the bundle early in the transient. The T = 50 s profile is the first to show any temperature rise in the unheated simulated fission gas plenum. As the transients proceeds and a flow is set up, the maximum temperature is swept to the end of the heated section. Loop temperatures for the entire two and a half hours of the transient are presented in Fig. 5B. The large thermal inertia of the expansion tank is readily apparent in the 20 - 40 minute time lag in the response of the thermocouple at its outlet. Large thermal perturbations are seen at the heat dump and pump. Recall that the trace heaters in the heat dump were switched off prior to the beginning of the test and with the large mass of the heat dump it appears a steady state condition did not exist at the beginning of the test.

The fact that a positive forced flow existed at the beginning of Test 35 is readily apparent in Figs. 6A and 6B. The peak bundle temperature is skewed downstream right from the beginning of the transient. The temperature drop across the heat dump at the beginning of the transient is consistent with this forced flow, although during the transition to natural convection there is again an apparent rise across the dump due to local transient effects.

In the parallel bundle test (Test 39) the temperature field development in the test section was very similar to that in Test 35 except that with a slightly lower bundle power the temperature levels were correspondingly lower. The loop transient temperature field is shown in Fig. 7. With both the test section and bypass open and the higher total heat input, the thermal effects are readily seen downstream earlier.

ANALYTICAL PROCEDURE

Analysis of the Bundle 6A natural convection tests has been based on use of LONAC[5], a one dimensional, single phase, finite-difference model for predicting THORS transients. The early version of this code had no provision for thermal inertia of piping and loop components such as the pump and included no thermal losses either. Inclusion of structure thermal inertia and piping losses and a fairly detailed model for the insulation and containment around the test bundle itself was essential to the simulation of the Bundle 6A tests. As noted earlier, sodium had permeated the insulation surrounding the test bundle and the resulting heat sink had to be fairly carefully modeled since it was in such close proximity to the pin bundle. Other structural components such as piping, the pump, expansion tank and heat exchanger were thermally modeled simply as single nodes in intimate contact with the adjacent sodium node [c.f. Ref. 11].

Since a fairly detailed discussion of the LONAC solution algorithm has been given previously[5] only a few points will be made here. The loop and bundle are divided into 36 energy nodes, 34 of which are of fixed volume. The other two represent the sodium in the pump bowl and expansion tank. The sodium levels in these two nodes are predicted by the code. Accurate prediction of these levels is particularly important because, for example, in the case of the pipe run between the expansion tank and pump bowl the temperature field in this line normally would tend to drive the flow in the negative direction were it not for the difference in free surface heights and in some cases argon pressurization in the expansion tank.

LONAC solves in sequence the one-dimensional conservation equations[12]:

$$\frac{A\partial\rho}{\partial\tau} + \frac{\partial(GA)}{\partial Z} = 0, \tag{1}$$

$$A\frac{\partial(\rho h)}{\partial\tau} + \frac{\partial M_s h_s}{\partial\tau} + \frac{\partial(GhA)}{\partial Z} = \phi, \tag{2}$$

$$A\frac{\partial G}{\partial\tau} + \frac{\partial}{\partial Z}\frac{G^2A}{\rho} = -A\frac{\partial p}{\partial Z} - K + \frac{fL}{d}\frac{|G|GA}{2\rho} - \rho gA, \tag{3}$$

where

A = cross-sectional area,

d = hydraulic diameter,

f = friction factor,

G = mass flow/area,

g = gravitational acceleration,

h = enthalpy,

h_s = enthalpy of structure

K = pressure drop coefficient,

L = length,

M_s = mass of structure,

p = pressure

Z = coordinate in flow direction,

ρ = density,

τ = time,

ϕ = heat source term.

A five node fuel pin radial heat conduction model is coupled to each sodium node in the heated zone. Similarly a five node radial conduction model for the insulation surrounding the test bundle and its containment (Fig. 2) is coupled to all test section axial nodes (both in the heated section and in the simulated fission gas plenum section). Runs were made using manufacturer's data for the insulation thermal properties and using estimated properties for the sodium-saturated insulation[9]. Other than in the test section, piping and other components were assumed to be at the same temperature as the contiguous sodium. Whereas for the large pipes used in a full scale reactor pipe heat capacity is less than half that of the contained sodium[13], pipe heat capacity ranges from 80 to 120% of the sodium in the small diameter pipes in THORS. The estimated or calculated masses of other loop components which were included in the thermal analysis were:

Heat dump (but not its support structure)	279 kg
Expansion tank	261 kg
Top and bottom flanges of test section	45 kg
Pump (impeller and bowl only)	241 kg

Losses from loop piping and other components were estimated using the results of the empty loop tests (Test 32) discussed earlier. An analytical determination of the heat losses would have been difficult if not impossible because of the large number of protuberances such as valves and flowmeters as well as the irregular geometry of elbows, tees and the pump. Using the Test 32 pipe temperatures and corresponding trace heater inputs an overall heat transfer coefficient can be obtained; that is,

$$H = \frac{q_{el}}{T_p - T_\infty}$$

where T_p is the temperature of the piping and T_∞ is the ambient temperature. By making the assumption that most of the resistance to heat transfer comes from the insulation around the pipe, this same coefficient may be used when sodium is flowing inside the pipe. Assuming that the coefficient is determined at T = 316°C, two terms are added to the energy balance. One is simply q_{el}, the trace heat input and the other represents the loss. The resultant is:

$$q_{el} - \frac{q_{el}(T - T_\infty)}{316 - T_\infty} = q_{el}\frac{(316 - T)}{(316 - T_\infty)}$$

As can be seen, if the sodium temperature at some position along the loop exceeds the reference temperature (316°C in this example), there will be some heat loss to the outside which is not compensated by the trace heater. If the sodium temperature is less than the reference temperature, then some of the trace heat is input to the sodium. Test 32 data can be found in Ref. 10.

The momentum equations are set up using the momentum integral method discussed by Meyer[14] and a staggered mesh. When the bypass line is open four separate momentum equations are written: one each for the main line from the pump to the tee, the bypass line from the tee to the expansion tank, the test section line from the tee to the expansion tank and the main line from the expansion

tank back through the heat dump to the pump bowl. These equations are algebraically manipulated to eliminate the pressure at the tee. The technique provides for transient flow redistribution due to different thermal heads in the bypass and the test section. With the bypass line closed, there are basically only two momentum equations to be solved. Data of Engel[15] were used for laminar and transition friction factors in the pin bundle. The stopped-rotor pressure drop of the pump was assumed to be neglible.

ANALYTICAL RESULTS

Simulations of Tests 35 and 39 were made using degraded test section insulation thermal properties. In addition, simulations were made using the Test 36B procedure with both degraded and "as built" insulation properties and several bundle powers in addition to the actual one. Weighted averages of the nearest experimentally measured temperatures were used to determine initial temperatures for each of the finite-difference volumes. In cases involving pressurization of the argon cover gas in the expansion tank (Test 35 and Test 39), it was assumed that when the two free surfaces were at the equilibrium no flow level and the loop was at 316°C (isothermal), then the cover gas pressure was 136 kPa (5 psig). Pressure changes due to heating or to volume changes could then be computed. This calculational procedure has some basis in the experimental procedure used and was necessitated by the lack at the time of pressure and temperature measuring devices in the cover gas space.

Test 36B was run from essentially a stopped flow condition. In the simulation of Test 36B (and the five other simulations based on the Test 36B procedure), a buoyancy-driven flow consistent with the experimentally-determined

initial loop temperature field was computed and used as the initial flow. This flow was less than a few percent of the flow which developed once the bundle heat was turned on. Figures 8A-C show the computed results. The temperature field in the test section (Fig. 8A) agrees reasonably well with experimental results (Fig. 5A) for the early part of the transient. Recall that the calculated temperature is a mean value for the bundle, whereas the experimental values are determined near the center of the bundle. For the long term transient (Figs. 5B and 8B) it is apparent that either the heat losses at the pump and heat dump are less than predicted or the heat capacity of these components is greater than that used in the calculation. The latter is highly likely because the value used for the mass of the heat dump did not include the massive support structure and the value used for the pump only included the rotor and bowl. The computed flow field (Fig. 8C) shows a gradual increase with a leveling off at about 1000 seconds into the transient. With friction and form losses orders of magnitude smaller than those of the main line through the bundle, the flow through the heat dump is far more oscillatory and shows the effects of sloshing between the two free surfaces.

When a run was made with Test 36B parameters but using "as built" test section insulation properties rather than the estimated degraded values, the results are dramatically different. With virtually all the generated heat going into the bundle rather than some leaking out through the insulation, temperatures rise dramatically and peak much sooner (Fig. 9A). The effect on the flow is even more dramatic (Fig. 9B). The flows rise quickly and overshoot before damping out.

To assess the effect of larger heat inputs on the flows and temperatures, runs were made at double and triple the test section power of Test 36B and with

both "as built" and degraded insulation thermal properties. Figure 10A shows the peak temperatures in the bundle and Fig. 10B shows the time to attain this peak temperature. The time plot is particularly revealing and shows an order of magnitude difference between "as built" and degraded insulation cases. Experimental results agree favorably with the 9.5 kW degraded insulation simulation results.

Test 35 was run from an initial low flow and with the cover gas equalization valve closed throughout the test. In the simulation a 0.13 ℓ/s (2 gpm) flow was established and then the pump head was instantaneously reduced to a null value. Test section temperatures (Fig. 11A) agree favorably with experimental values [Fig. 6A]. The computed flows are shown in Fig. 11A. Note that the two flows are equal at $\tau = 0$, but being directly coupled to the pump, the test section flow drops quickly in the first second. As the test section heats up, the flow increases gradually and levels off at $\tau \sim 1000$ sec.

In Test 39 the bypass line was open. Under isothermal conditions the bypass line valve was adjusted to give approximately 0.13 ℓ/s (2 gpm) through both the bypass and test section. In the simulation the bypass valve setting was arrived at by an iterative procedure but using the actual temperature field which existed in the bundle and bypass at the start of the test. Since this field corresponded to a power-on low forced flow situation there would be some buoyancy effects in both the analytically determined valve settings and pump head. Results for the test section temperature field and the predicted flows are shown in Figs. 12A and 12B. The flow is particularly interesting because the experimental procedure for this run involved a simultaneous pump shutdown and expansion tank cover gas depressurization. The effects are particularly apparent in the lightly damped line through the heat dump. The experimental heat input

to the test section was about 10% higher than that of the trace heaters to the bypass line and so higher higher flows are computed in the latter. Some difference in the transient behavior of the test section and that of the bypass at low flow conditions is explained by the fact that pressure drop in the bundle at laminar flow conditions is linear in flow while that across the bypass valve (pipe friction is small) was considered proportional to flow squared even at very low flows.

CONCLUSIONS

As can be seen in Fig. 10A, fairly good agreement was obtained between experimentally measured and LONAC-predicted peak temperatures. The temperature profiles early in the transient were also fairly well-matched by the code. Some reasons for this success and other observations will be discussed in this section.

In a large-scale reactor the sodium flow on the primary side of the intermediate heat exchanger (IHX) is in the vertical direction and involves a substantial elevation change over the length[13]. In contrast the sodium flow through the THORS Na-air 0.5MW heat dump is in nearly the horizontal direction. Thus the crudeness of the heat dump thermal model is not felt until the thermal pulse reaches a vertical leg. Further refinement of the heat dump model would be difficult because with the blower off and the damper closed, the heat dump was operating at only a few percent of its design rating. As noted earlier trace heaters on the heat dump tubes and supplementary radiator heaters were off during these tests. A more sophisticated model would also have to include at least part of the massive heat dump support structure. Sodium flow in the new 2.0 MW heat dump to be used for future THORS tests with larger bundles will be upward rather than downward as in the primary side of a reactor IHX.

For similar reasons the crude pump thermal model does not affect the early part of the transient. Future THORS natural convection tests would involve a new electromagnetic pump which will be located in a vertical piping leg.

As can be seen from Figs. 10A and 10B, the thermal properties of the insulation surrounding the test bundle play a dominant role in the transient. Manufacturer's data was available for the "as built" insulation, but the properties

of the degraded insulation could only be estimated. The manufacturer's data indicated that the porosity of the material was 53%. Under the assumption that all pore space was full of sodium, a thermal conductivity which was 53% that of pure sodium (and over 200 times that of the "as built" insulation) was used for the degraded insulation. Similarly the heat capacity was computed on the basis of 53% sodium and 47% insulation. Clearly the agreement (or disagreement) between experimental and LONAC values seen in Figs. 10A and 10B is a strong function of this assumption. In a full-scale reactor the thick hexcan wall and cooler adjacent subassemblies would have important effects as heat sinks during a slow natural convection transient.

The pressure drop in the bundle was orders of magnitude larger than that in the rest of the loop except in Test 39 where the valve in the bypass was adjusted to give a pressure drop nearly equal to that across the test section at equal flows. Under the decay heat conditions simulated here the flow in the bundle is in the laminar and transition regimes. This is also the case for the full-scale reactor under decay heat conditions; but in the reactor many more, larger assemblies feed the also larger loop piping. The result is that in THORS the flow in the loop piping is in the laminar and potentially troublesome-to-evaluate transition regimes, while that in reactor piping would be well into the turbulent regime. Again because the bulk of the pressure drop is in the bundle where apparently it has been well-modeled using the Engel et al.[15] results, the LONAC simulation appears not to suffer. Similarly the neglect of the pump stopped-rotor pressure drop seems not to be a problem in THORS.

The THORS tests discussed in these tests have generated a wealth of loop and intra-assembly data under simulated decay heat conditions. They have demonstrated the ability of a simplified computer code to model the THORS loop,

the design of which nearly a decade ago included little consideration of transient testing at all, let alone testing under natural convection conditions. The tests and analysis discussed here have given insights which will be helpful in planning future tests under natural convection conditions and insights which will help in code improvements for simulating long transients.

Appendix

THORS BUNDLE 6A NATURAL CONVECTION TEST SUMMARY

TEST NO	DATE	INITIAL FLOW	TEST SECTION VALVE (HV-273)	BYPASS VALVE (HV-258)	EQUALIZATION VALVE (HV-259)	INLET TEMP (C)	TEST SECTION HEAT (KW)	TRACE HOT LEG (C)	HEAT COLD LEG (C)	NOTES
35	1-17-77	FORCED .13L/S	OPEN	CLOSED	CLOSED	316.	9.0 UNIFORM	482.	316.	
36	1-18-77	STOPPED	OPEN	CLOSED	CLOSED	316.	9.0 UNIFORM	482.	316.	
36A	1-20-77	STOPPED	OPEN	CLOSED	OPEN	316.	9.5 UNIFORM	482.	316.	ONE SET TRACE HEATERS BAD
36B	1-21-77	STOPPED	OPEN	CLOSED	OPEN	316.	9.5 UNIFORM	316.	316.	
37	1-19-77	FORCED .13L/S	OPEN	CLOSED	CLOSED	316.	9.5 80% SKEW	482.	316.	PROCEDURE SAME AS 35
38	1-19-77	STOPPED	OPEN	CLOSED	CLOSED	316.	9.5 80% SKEW	482.	316.	PROCEDURE SAME AS 36
39	1-24-77	FORCED .13L/S	OPEN	OPEN	OPEN	316.	7.3 UNIFORM	482.	316.	BYP VALVE ADJUSTED TO GIVE .13L/S BYP FLOW 6.6 KW TRACE HEAT ON BYPASS

IFC0121 STOP 0

ACKNOWLEDGMENTS

The author wishes to acknowledge the vital roles of Dr. M. H. Fontana, Head of the Advanced Reactor Systems Section; Dr. J. L. Wantland, Manager of the THORS Project Planning and Analysis Staff and P. A. Gnadt, Manager of the THORS Project Construction and Operation Staff as well as the efforts of N. E. Clapp, N. Hanus and W. R. Nelson of the THORS Staff. This research has been supported by the U.S. Department of Energy under Contract No. W-7405-eng-26.

References

1. Additon, S. L., and Parziale, E. A., "Natural Circulation in FFTF, A Loop Type LMFBR," Symposium on the Thermal and Hydraulic Aspects of Nuclear Reactor Safety, Vol. 2, Liquid Metal Fast Breeder Reactors, ASME, 1977, p. 265-283.

2. Singer, R. M., Grand, D., and Martin, R., "Natural Circulation Heat Transfer in Pool-Type LMFBR's," Symposium on the Thermal and Hydraulic Aspects of Nuclear Reactor Safety, Vol. 2, Liquid Metal Fast Breeder Reactors, ASME, 1977, pp. 239-264.

3. "LMFBR Demonstration Plant Simulation Model (DEMO)," WARD-D-0005, Rev. 4, Jan. 1976.

4. Coffield, R. D. et al., "LMFBR Natural Circulation Verification Program (NCVP) Review of Experimental Facilities and Testing Recommendations," WARD-NC-3045-1, July 1977.

5. Ribando, R. J., "LONAC: A Computer Program to Investigate Systems Dynamics Under Conditions of Low Forced Flow and Natural Convection," ORNL/TM-6228, April 1978.

6. Fontana, M. H. et al., "Temperature Distribution in a 19-Rod Simulated LMFBR Fuel Assembly in a Hexagonal Duct (Fuel Failure Mockup Bundle 2A) - Record of Experimental Data," ORNL/TM-4113, September 1973.

7. Wantland, J. L. et al., "Sodium Boiling Tests in a 19-Rod Bundle with a Central Blockage - Record of Experimental Data for Fuel Failure Mockup Bundle 3B, ORNL/TM-5458, October 1976.

8. Wantland, J. L. et al., "Steady-State Sodium Tests in a 19-Pin Full-Length Simulated LMFBR Fuel Assembly - Record of Steady State Experimental Data for THORS Bundle 6A," ORNL/TM-6106, March 1978.

9. Ribando, R. J. et al., "Sodium Boiling in a Full-Length 19-Pin Simulated Fuel Assembly (THORS Bundle 6A)," ORNL/TM-6553, January 1979.

10. Ribando, R. J. et al., "A Comparison of Numerical Results with Experimental Data for Single-Phase Natural Convection in an Experimental Sodium Loop," ORNL/TM-6778 (to be published).

11. Planchon, H. P. and Laster, W. R., "Loop Heat Capacity Models and Their Effects for DEMO Natural Circulation Transient Analysis," WARD-NC-3045-2, September 1978.

12. Meyer, J. E., "Conservation Laws in One-Dimensional Hydrodynamics," Bettis Technical Review, WAPD-BT-20, September 1960, pp. 61-72.

13. "Clinch River Breeder Reactor Plant Project Design Description," CRBRP-PMC-77-06.

14. Meyer, J. E. and Rose, R. P., "Application of a Momentum Integral Model to the Study of Parallel Channel Boiling Oscillations," Journal of Heat Transfer, Trans. ASME, Series C, Vol. 85, 1963, pp. 1-9.

15. Engel, F. C., Markley, R. A., and Bishop, A. A., "Laminar, Transition and Turbulent Parallel Flow Pressure Drop Across Wire Wrap Spaced Rod Bundles," Nuclear Science and Engineering, Vol. 69, No. 2, February 1979, p. 290.

Figure Captions

Figure 1. Isometric drawing of the THORS Facility for Bundle 6A operation. Note that the pipe run containing the old test section was shut off during all tests.

Figure 2. Cross section of Bundle 6A.

Figure 3. Bundle 6A fuel pin simulator.

Figure 4. THORS Bundle 6A test-section assembly showing axial dimensions. (1 in. = 25.4 mm).

Figure 5A. Temperatures recorded along the bundle axis plotted at selected times early in the transient. [THORS Bundle 6A, Test 36B (no initial forced flow).]

Figure 5B. Temperatures recorded around the THORS loop plotted at selected times during the transient [THORS Bundle 6A, Test 36B (no initial forced flow)].

Figure 6A. Temperatures recorded along the bundle axis plotted at selected times early in the transient. [THORS Bundle 6A, Test 35 (initial low forced flow).]

Figure 6B. Temperatures recorded around the THORS loop plotted at selected times during the transient. [THORS Bundle 6A, Test 35 (initial low forced flow)].

Figure 7. Temperatures recorded around the THORS loop plotted at selected times during the transient. [THORS Bundle 6A, Test 39 (parallel assembly test)].

Figure 8A. Computed test section temperatures for various times early in the transient. LONAC simulation of THORS Bundle 6A, Test 36B.

Figure 8B. Computed loop temperatures for various times during the transient. LONAC simulation of THORS Bundle 6A, Test 36B.

Figure 8C. Computed flows versus time. LONAC simulation of THORS Bundle 6A, Test 36B.

Figure 9A. Computed test section temperatures for various times early in the transient. LONAC simulation of THORS Bundle 6A, Test 36B but with "as built" insulation.

Figure 9B. Computed flows versus time. LONAC simulation of THORS Bundle 6A, Test 36B but with "as built" insulation.

Figure 10A. Maximum temperature measured in the bundle at any time during the transient for THORS Bundle 6A, Tests 35, 36B and 39 compared with LONAC predictions for these cases and hypothetical cases using the Test 36B procedure.

Figure 10B. Time calculated to reach the peak temperatures plotted in Fig. 10A. LONAC simulation using Test 36B procedure, both with "as built" and degraded insulation and with actual and higher bundle powers.

Figure 11A. Computed test section temperatures for various times early in the transient. LONAC simulation of THORS Bundle 6A, Test 35 (low initial forced flow).

Figure 11B. Computed flows versus time. LONAC simulation of THORS Bundle 6A, Test 35 (low initial forced flow).

Figure 12A. Computed test section temperatures for various times early in the transient. LONAC simulation of THORS Bundle 6A, Test 39 (parallel assembly test).

Figure 12B. Computed flows versus time. LONAC simulation of THORS Bundle 6A, Test 39 (parallel assembly test).

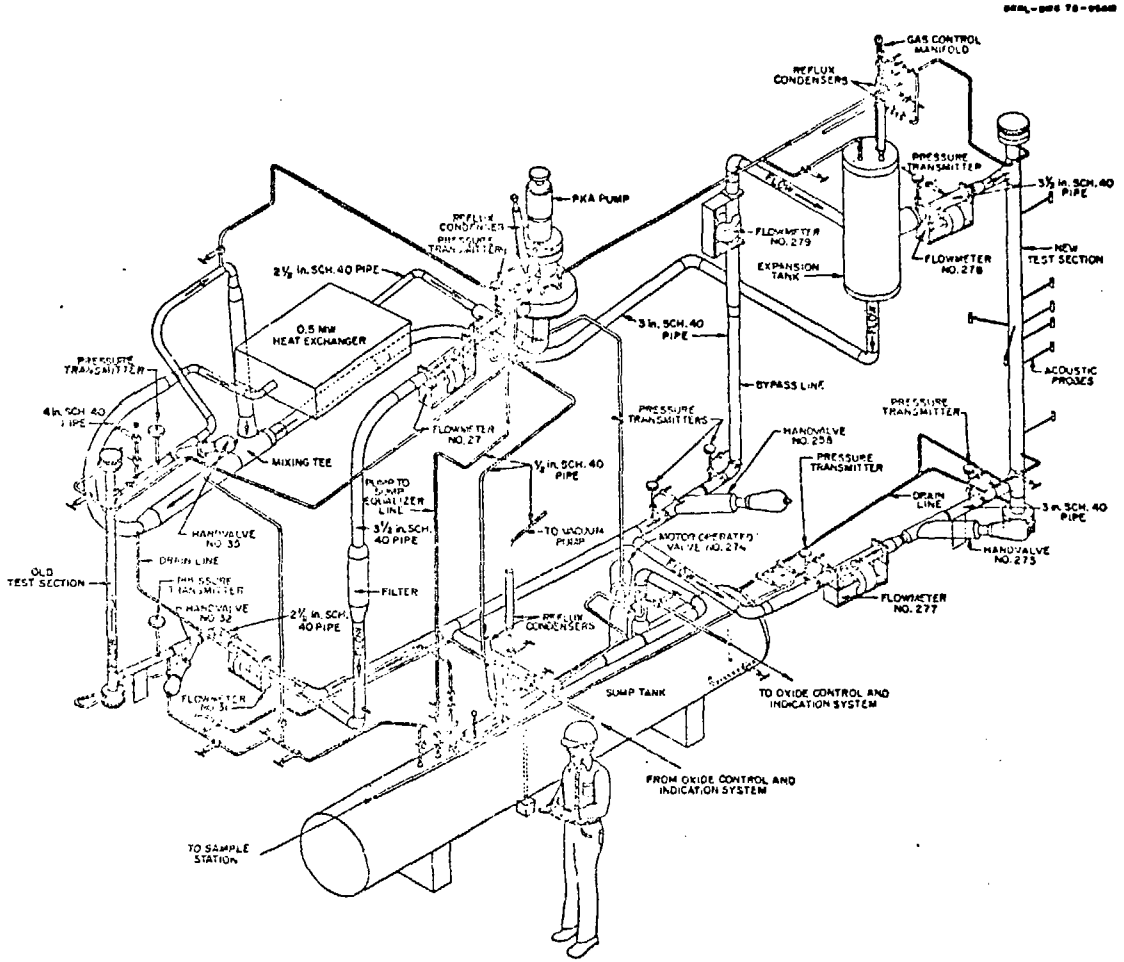

Figure 1. Isometric drawing of the THORS Facility for Bundle 6A operation. Note that the pipe run containing the old test section was shut off during all tests.

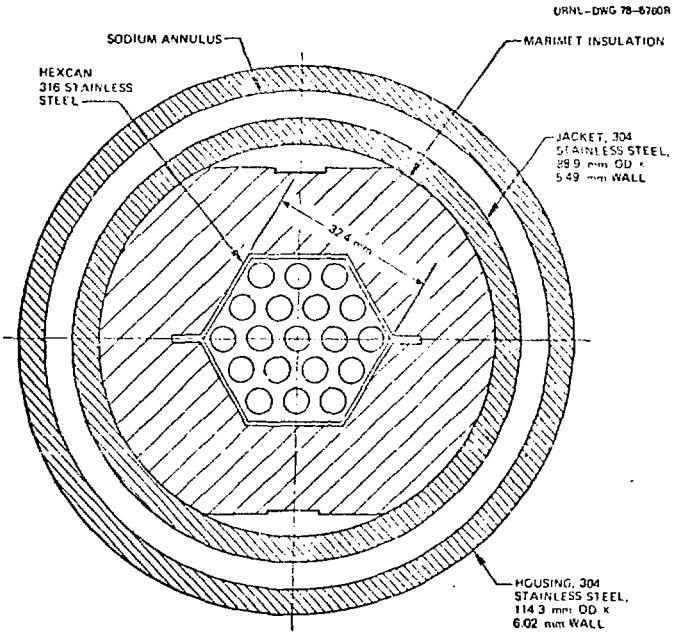

Figure 2. Cross section of Bundle 6A.

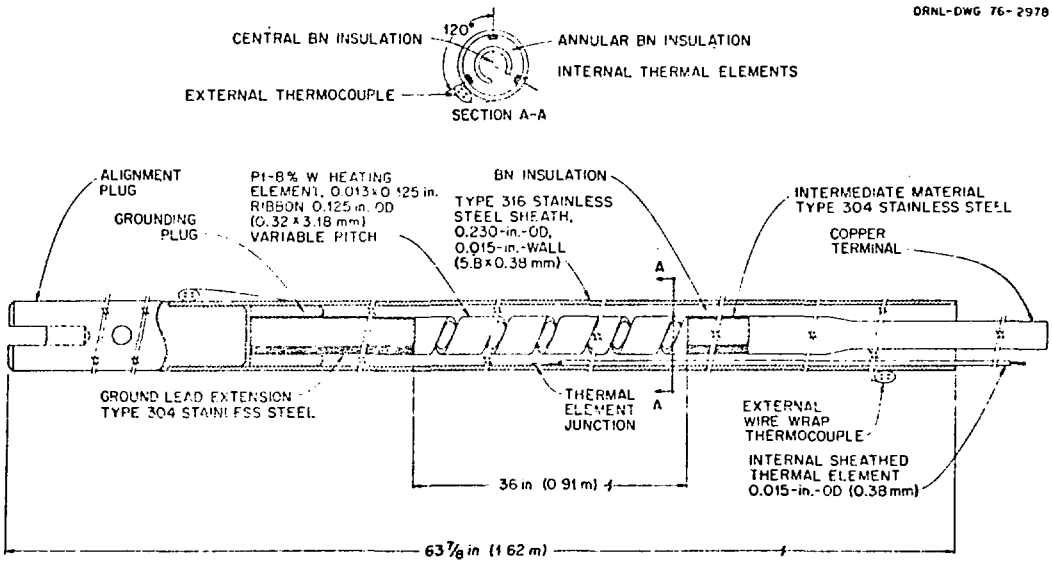

Figure 3. Bundle 6A fuel pin simulator.

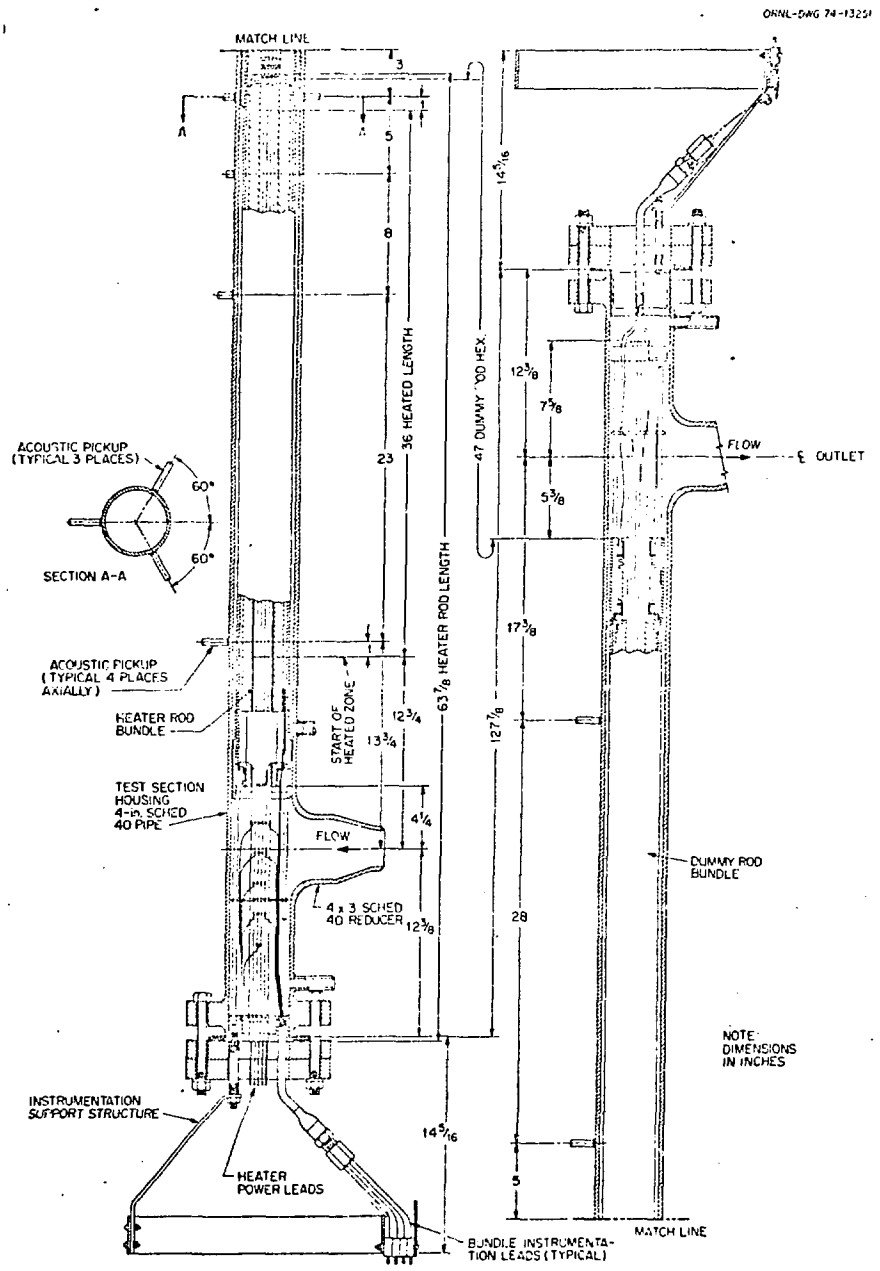

Figure 4. THORS Bundle 6A test-section assembly showing axial dimensions. (1 in. = 25.4 mm).

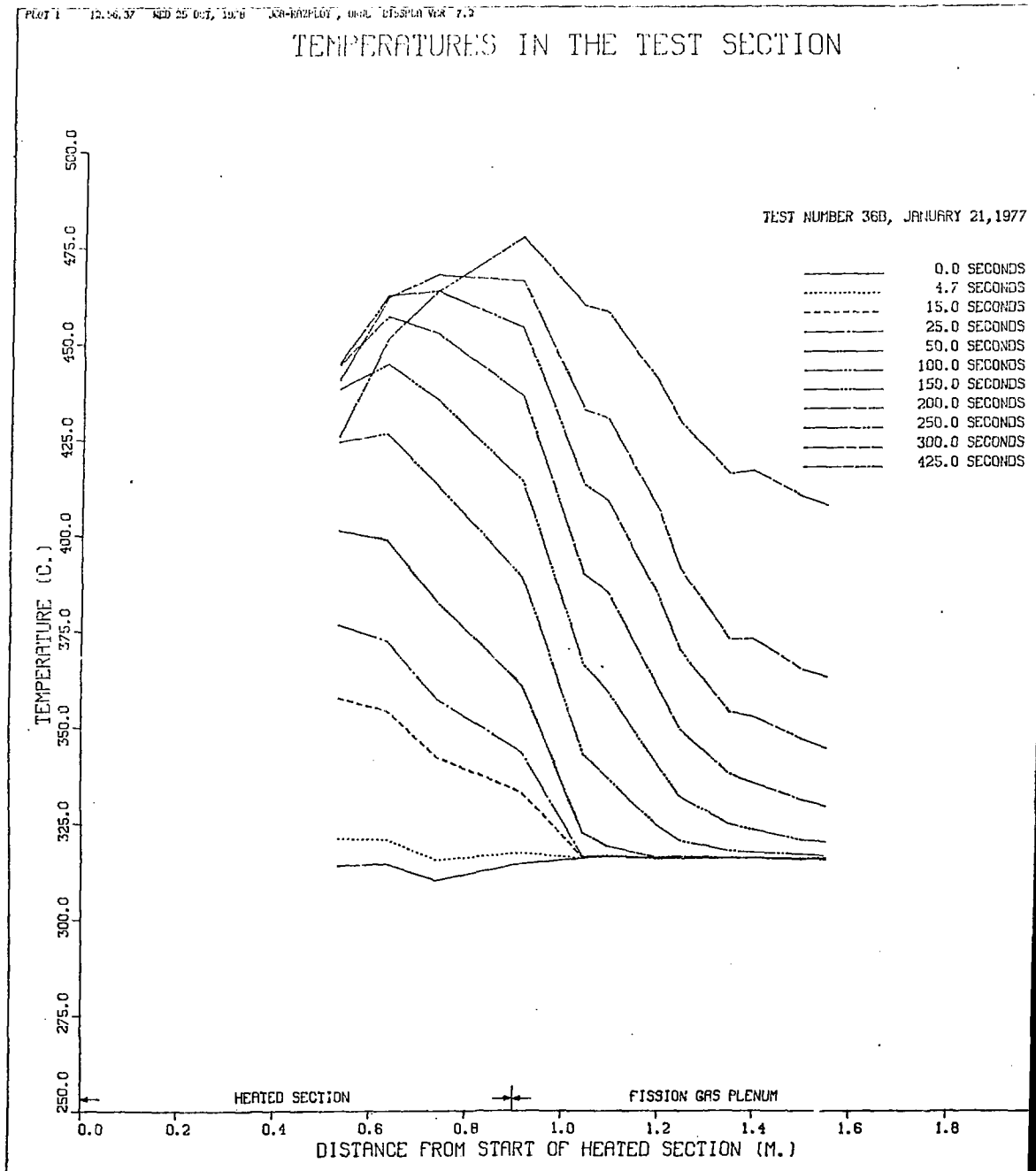

Figure 5A. Temperatures recorded along the bundle axis plotted at selected times early in the transient. [THORS Bundle 6A, Test 36B (no initial forced flow).]

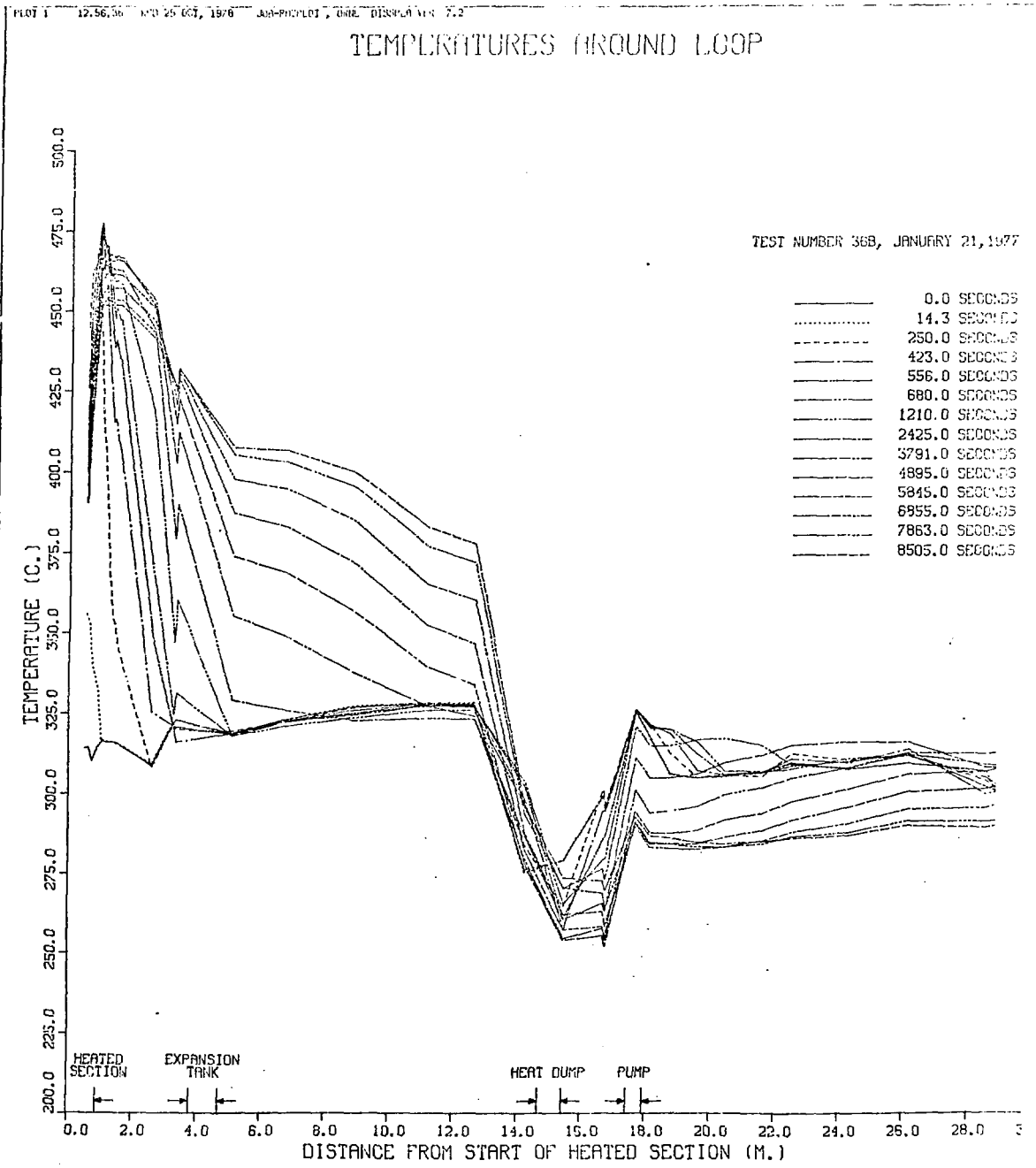

Figure 5B. Temperatures recorded around the THORS loop plotted at selected times during the transient [THORS Bundle 6A, Test 36B (no initial forced flow)].

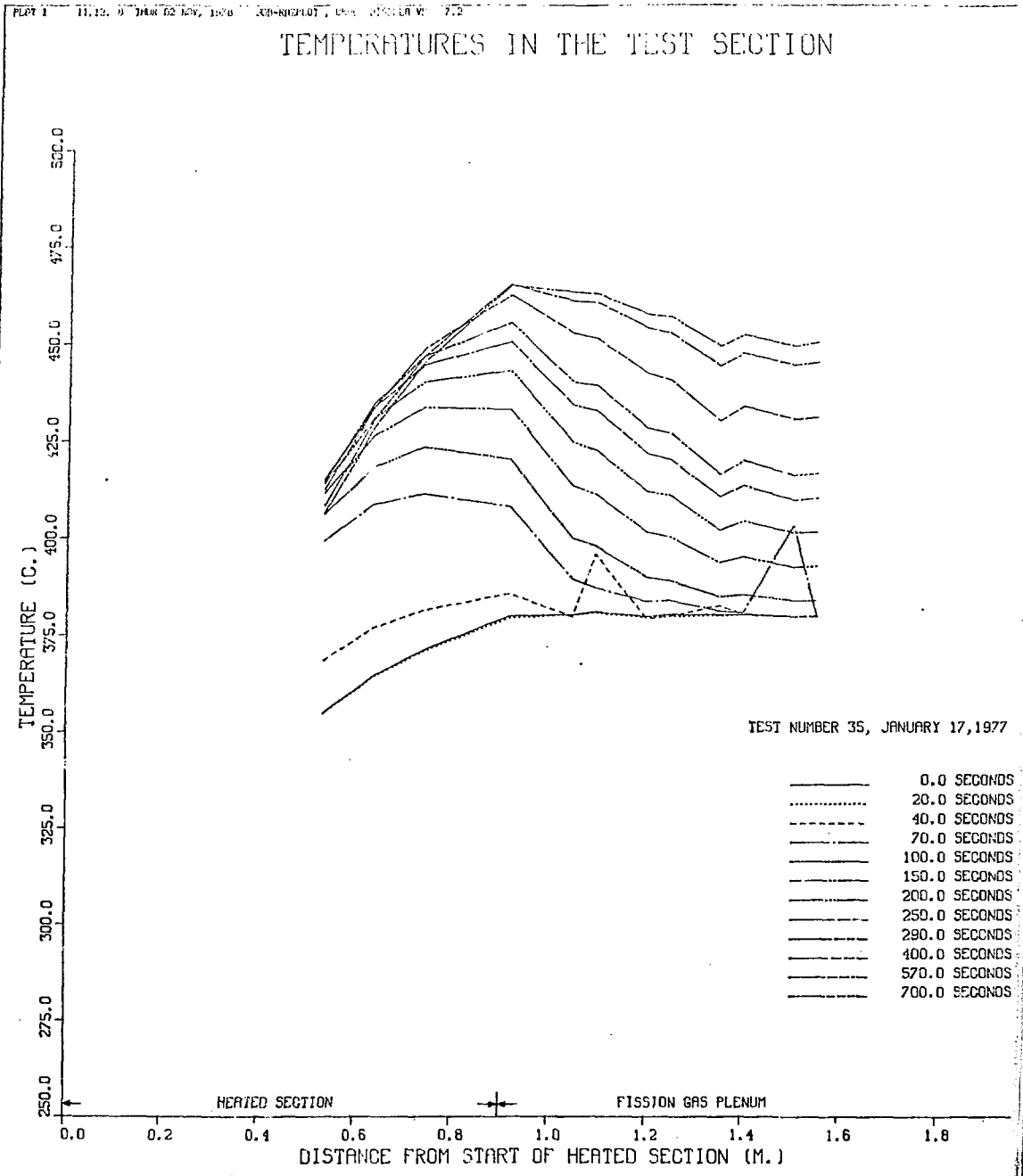

Figure 6A. Temperatures recorded along the bundle axis plotted at selected times early in the transient. [THORS Bundle 6A, Test 35 (initial low forced flow).]

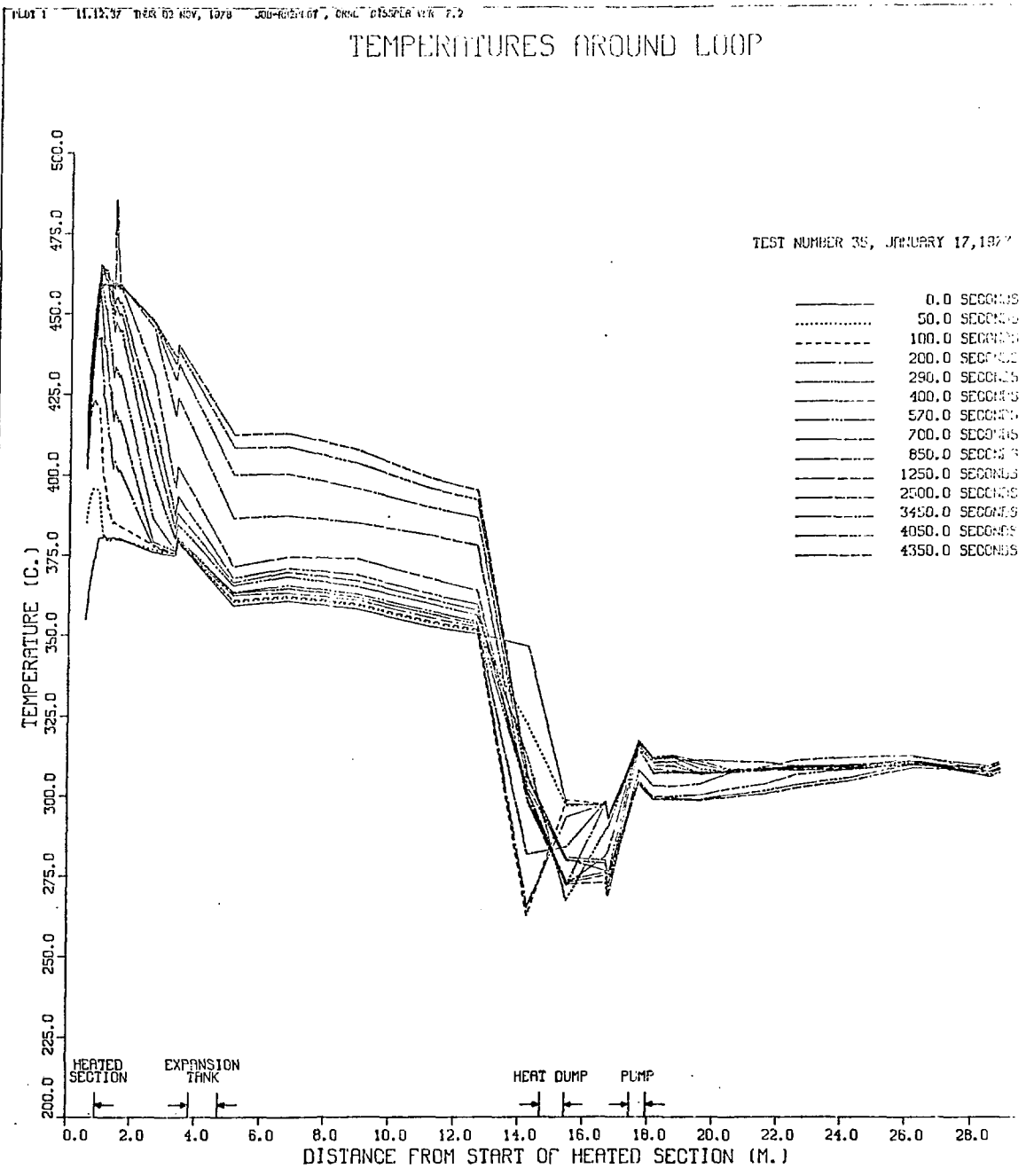

Figure 6B. Temperatures recorded around the THORS loop plotted at selected times during the transient. [THORS Bundle 6A, Test 35 (initial low forced flow)].

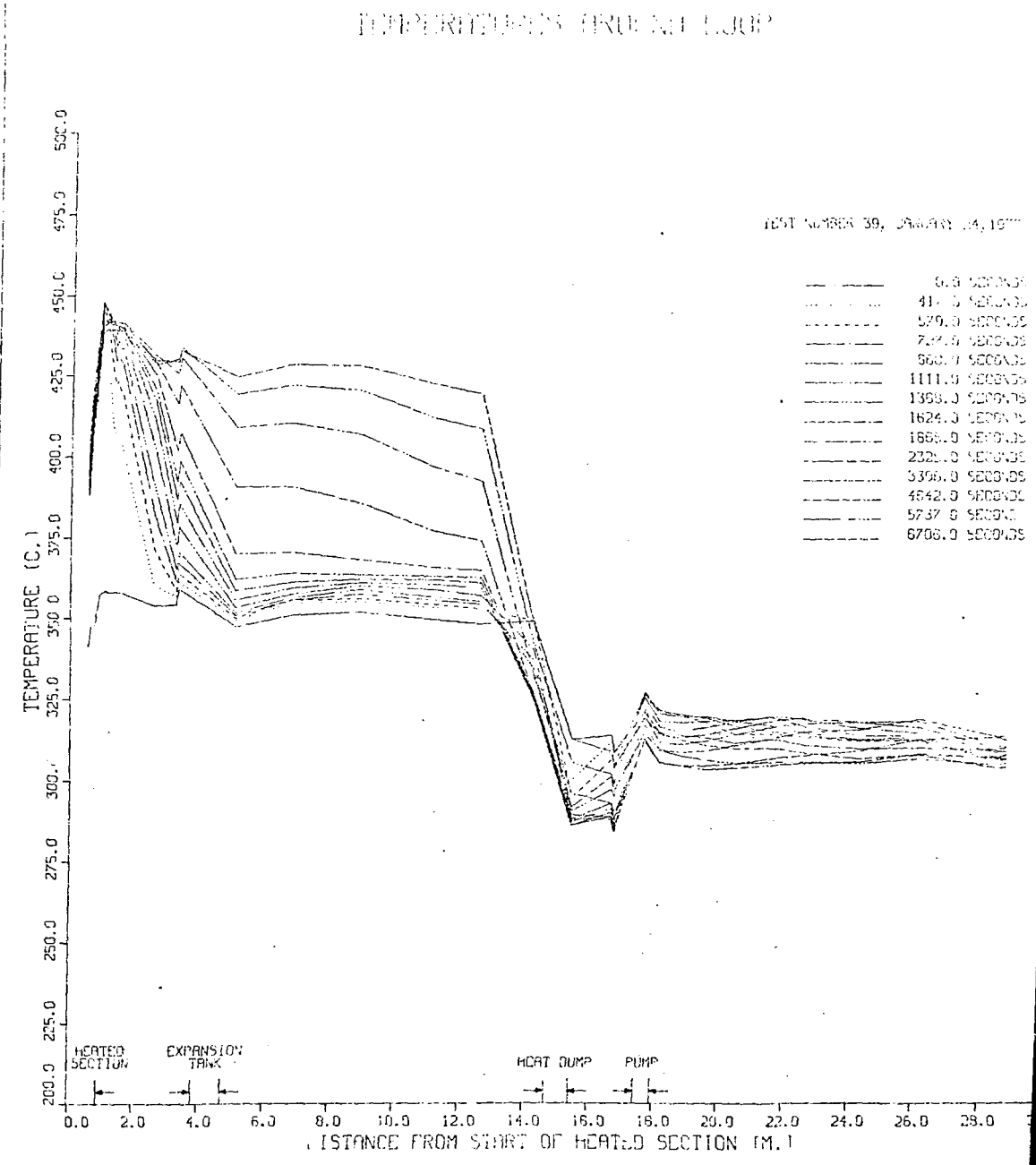

Figure 7. Temperatures recorded around the THORS loop plotted at selected times during the transient. [THORS Bundle 6A, Test 39 (parallel bundle test)].

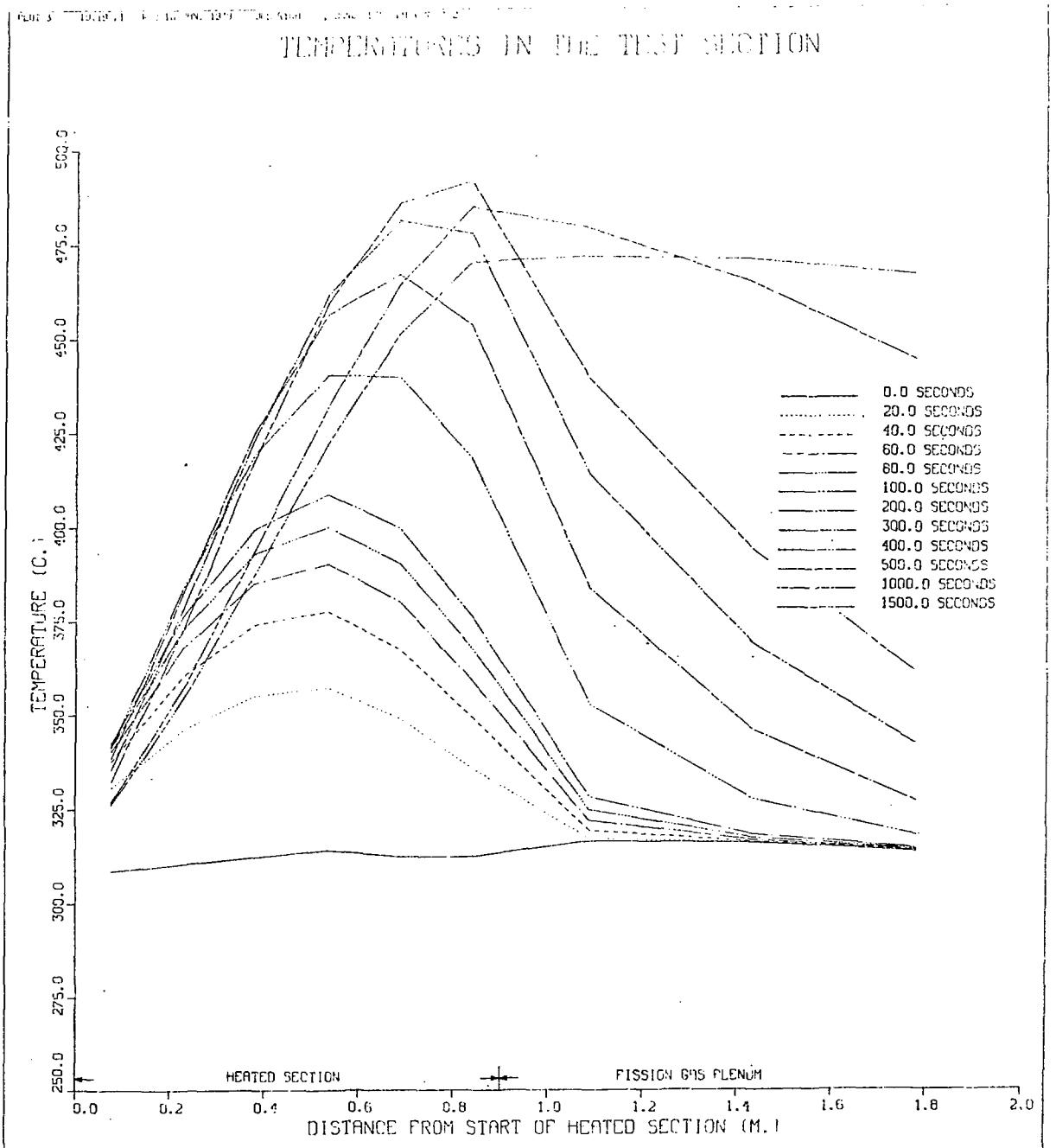

Figure 8A. Computed test section temperatures for various times early in the transient. LONAC simulation of THORS Bundle 6A, Test 36B.

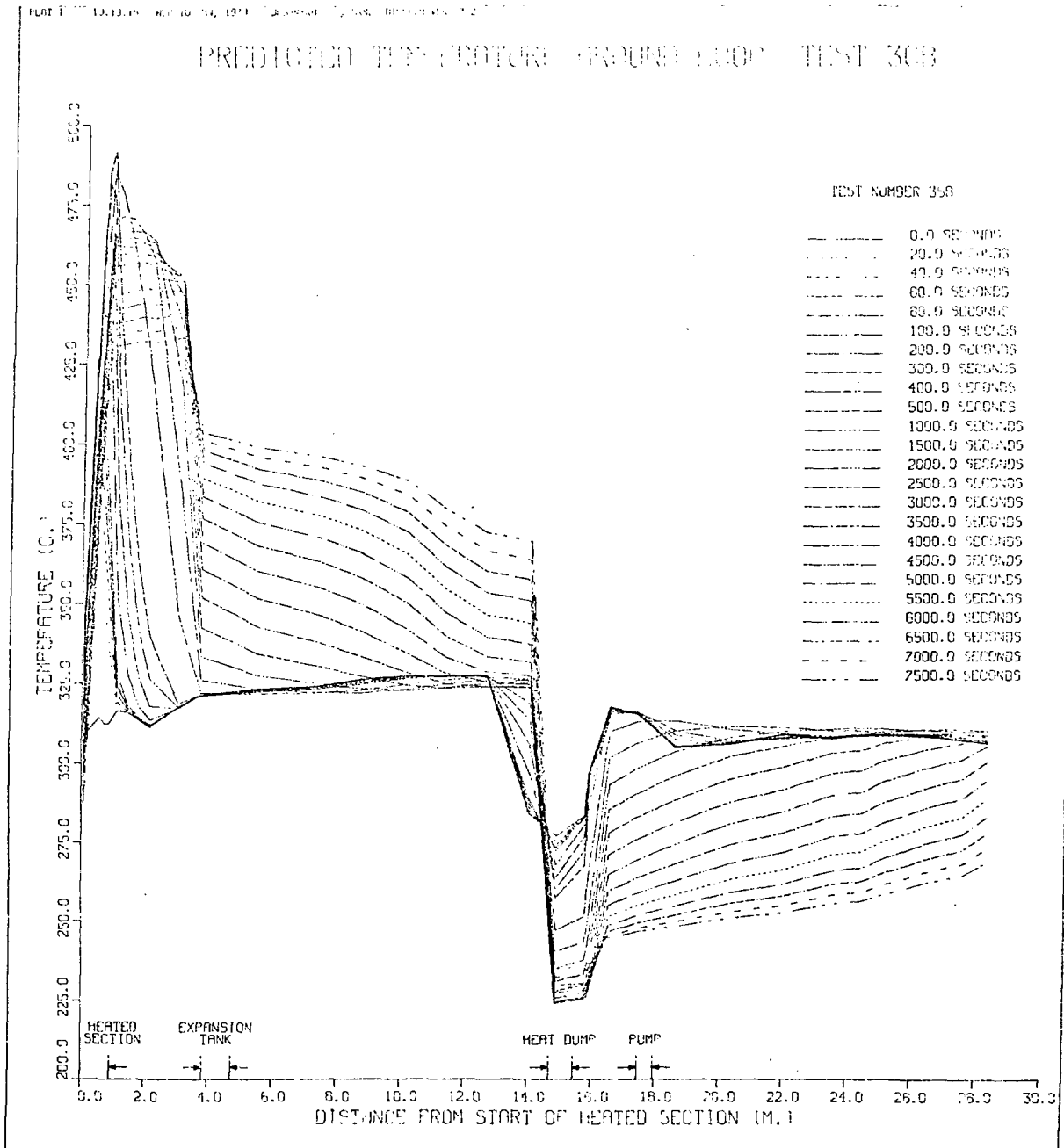

Figure 8B. *Computed loop temperatures for various times during the transient. LONAC simulation of THORS Bundle 6A, Test 36B.*

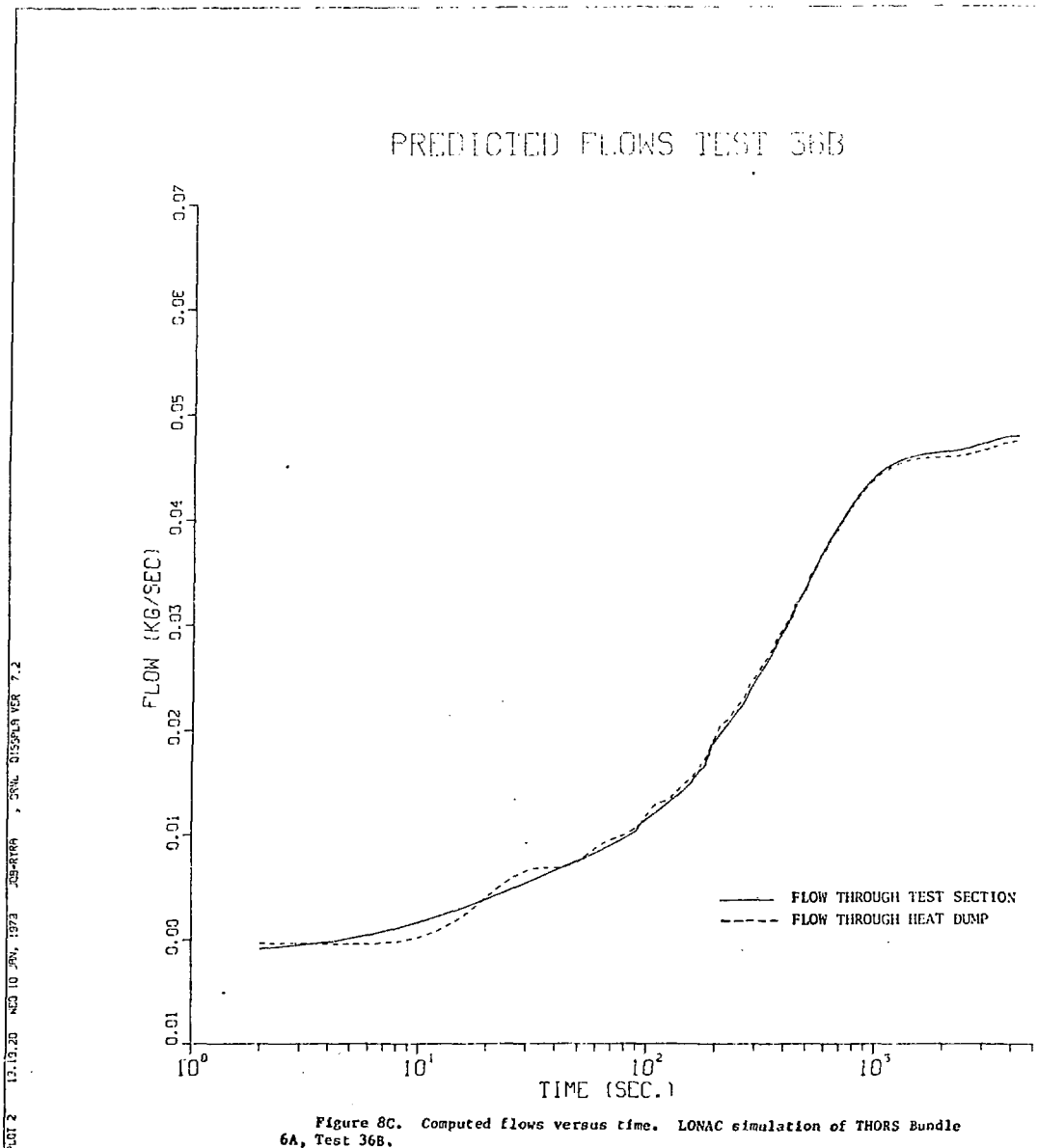

Figure 8C. *Computed flows versus time. LONAC simulation of THORS Bundle 6A, Test 36B.*

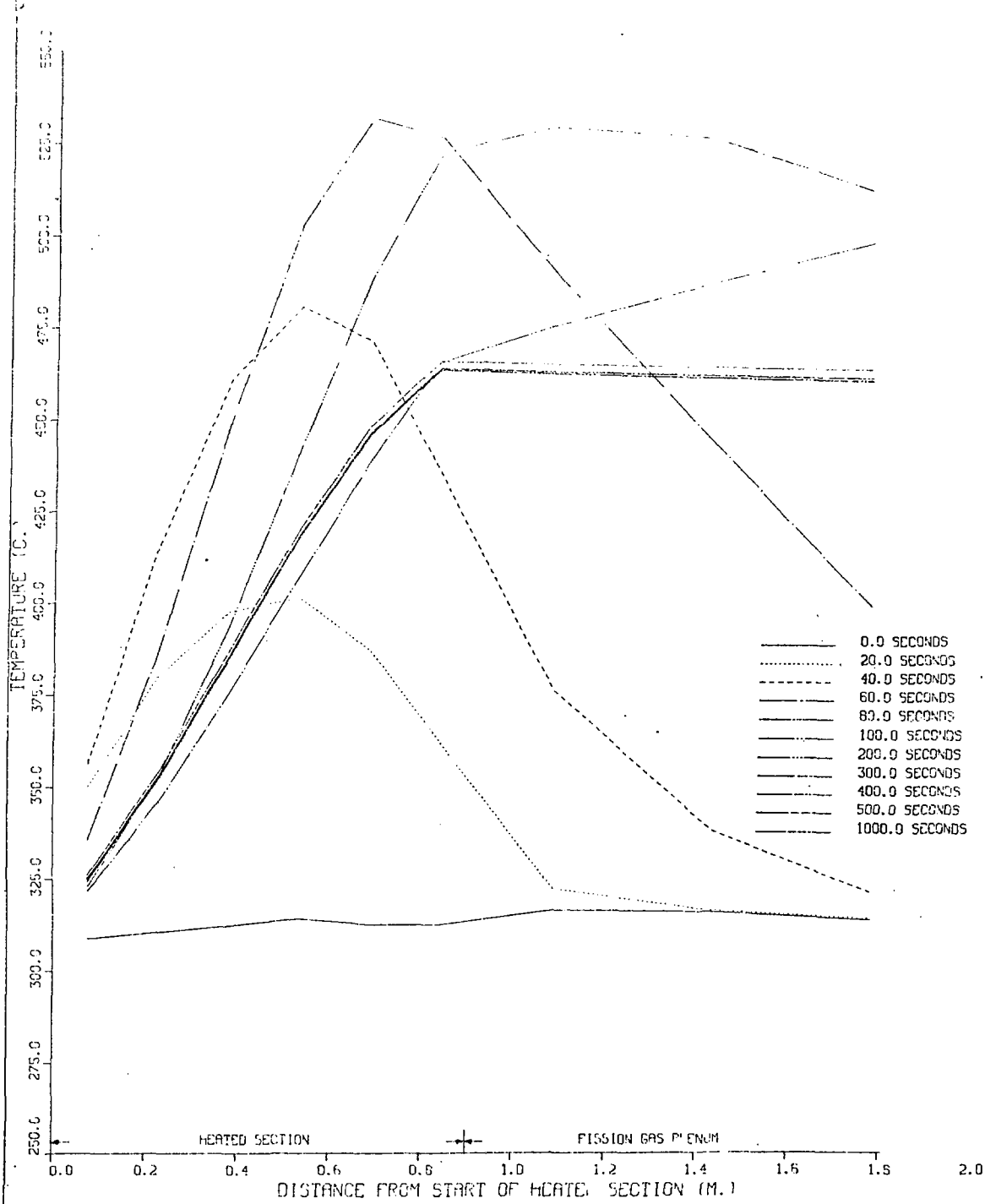

Figure 9A. Computed test section temperatures for various times early in the transient. LONAC simulation of THORS Bundle 6A, Test 36B but with "as built" insulation.

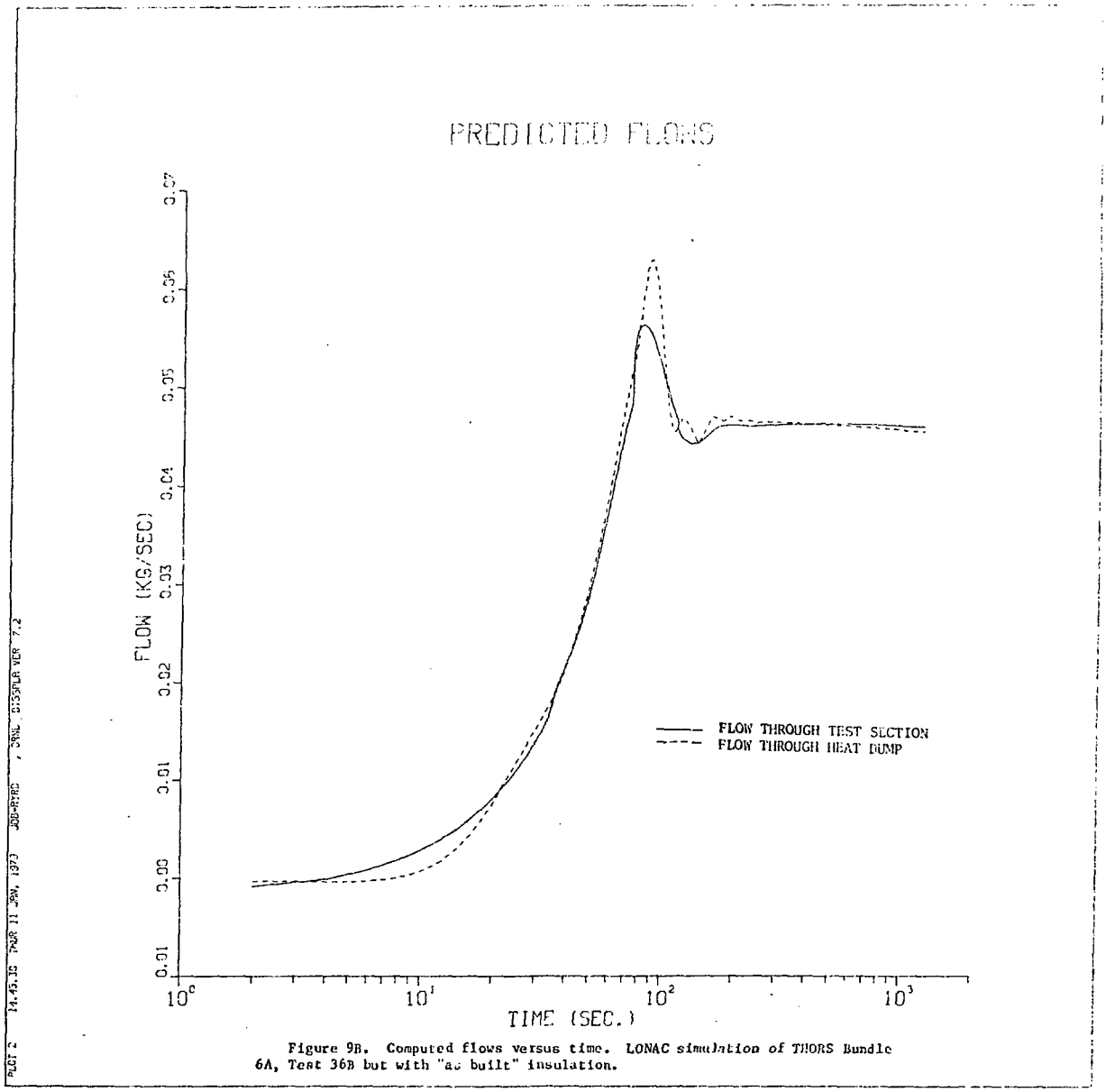

Figure 9B. Computed flows versus time. LONAC simulation of THORS Bundle 6A, Test 36B but with "as built" insulation.

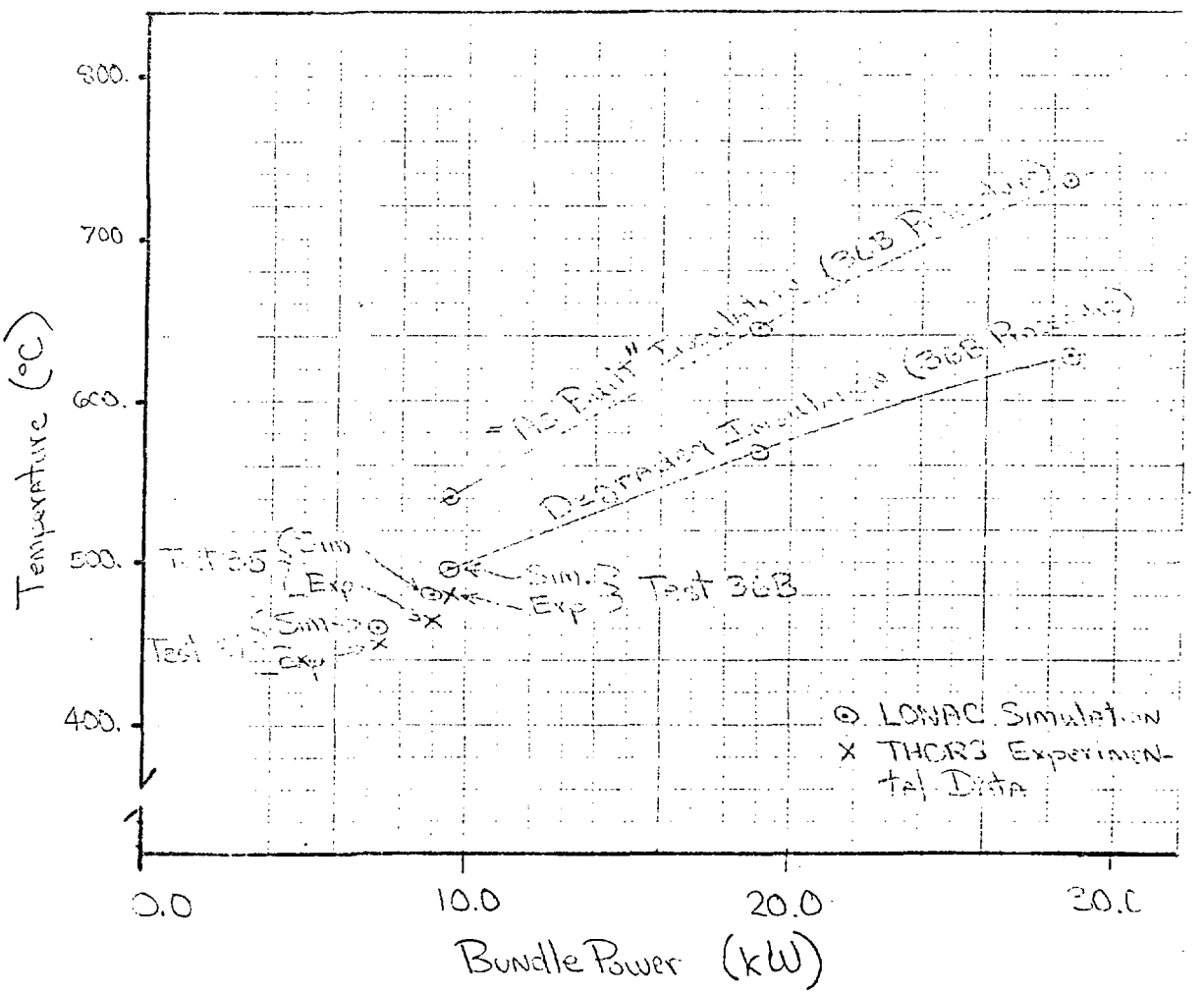

Figure 10A. Maximum temperature measured in the bundle at any time during the transient for THORS Bundle 6A, Tests 35, 36B and 39 compared with LONAC predictions for these cases and hypothetical cases using the Test 36B procedure.

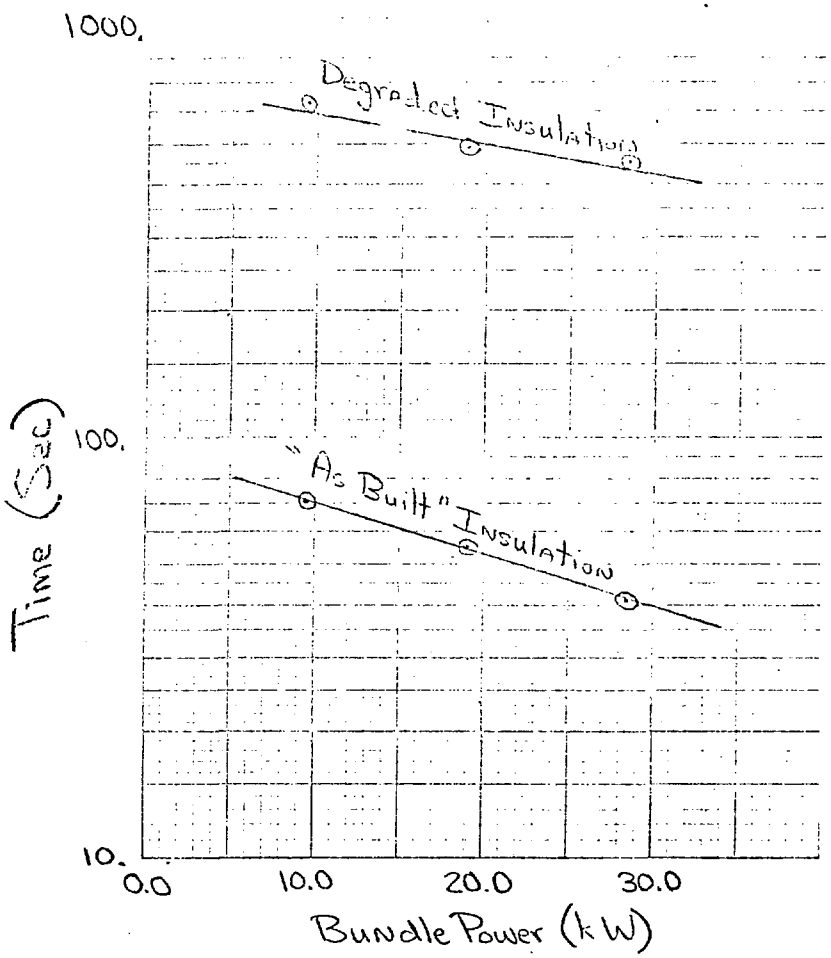

Figure 10B. . Time calculated to reach the peak temperatures plotted in Fig. 10A. LONAC simulation using Test 36B procedure, both with "as built" and degraded insulation and with actual and higher bundle powers.

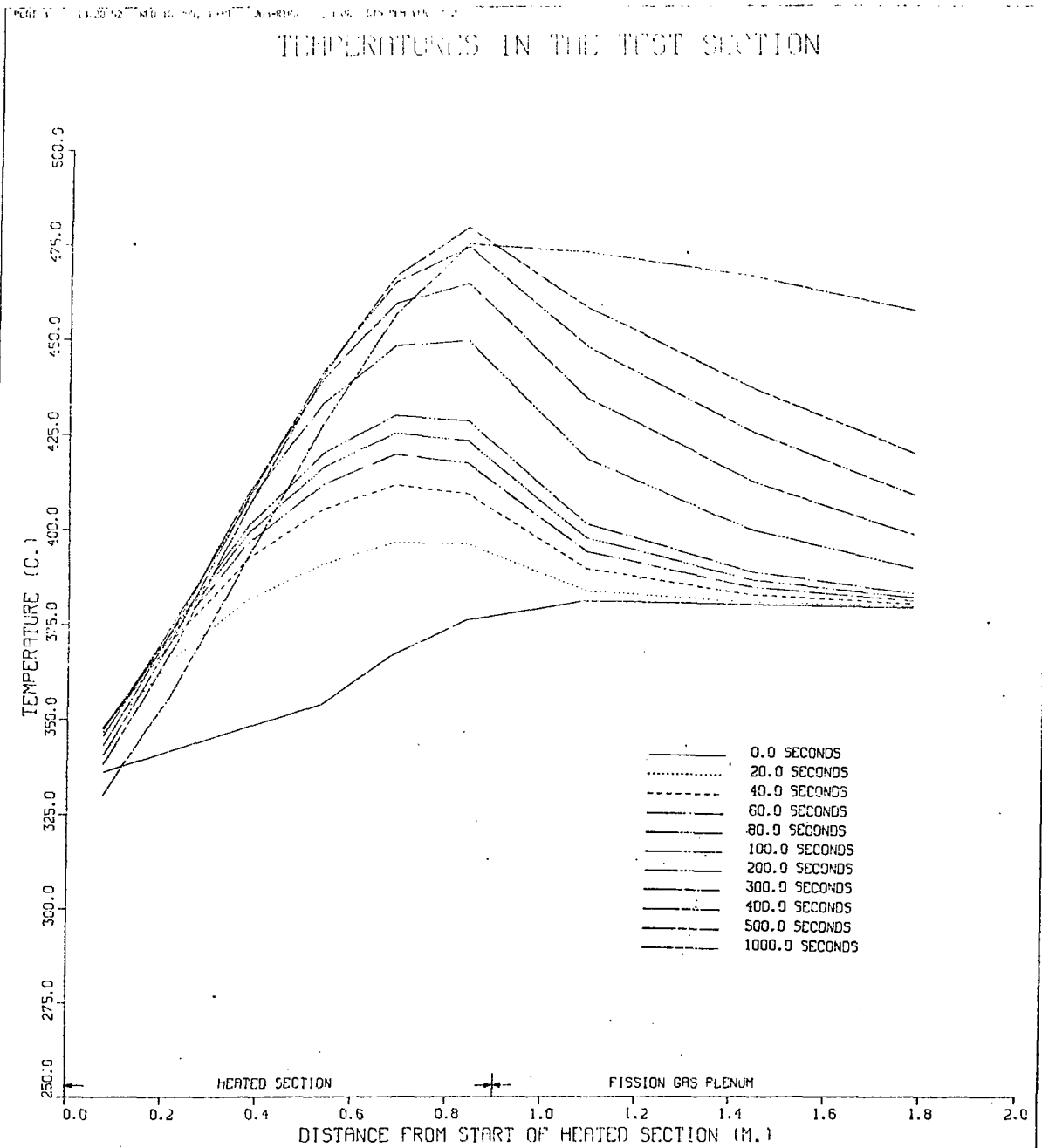

Figure 11A. Computed test section temperatures for various times early in the transient. LONAC simulation of THORS Bundle 6A, Test 35 (low initial forced flow).

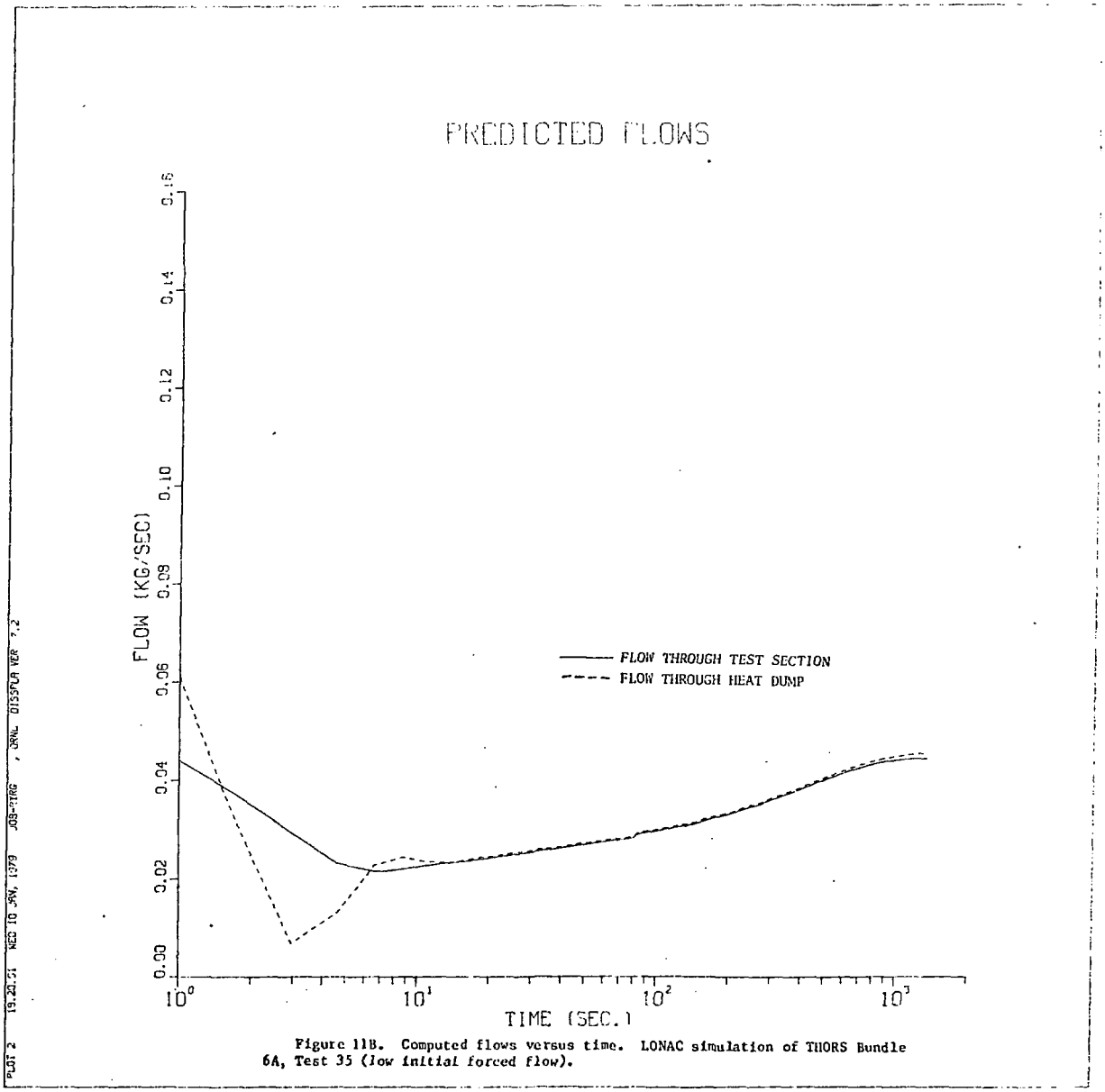

Figure 11B. Computed flows versus time. LONAC simulation of THORS Bundle 6A, Test 35 (low initial forced flow).

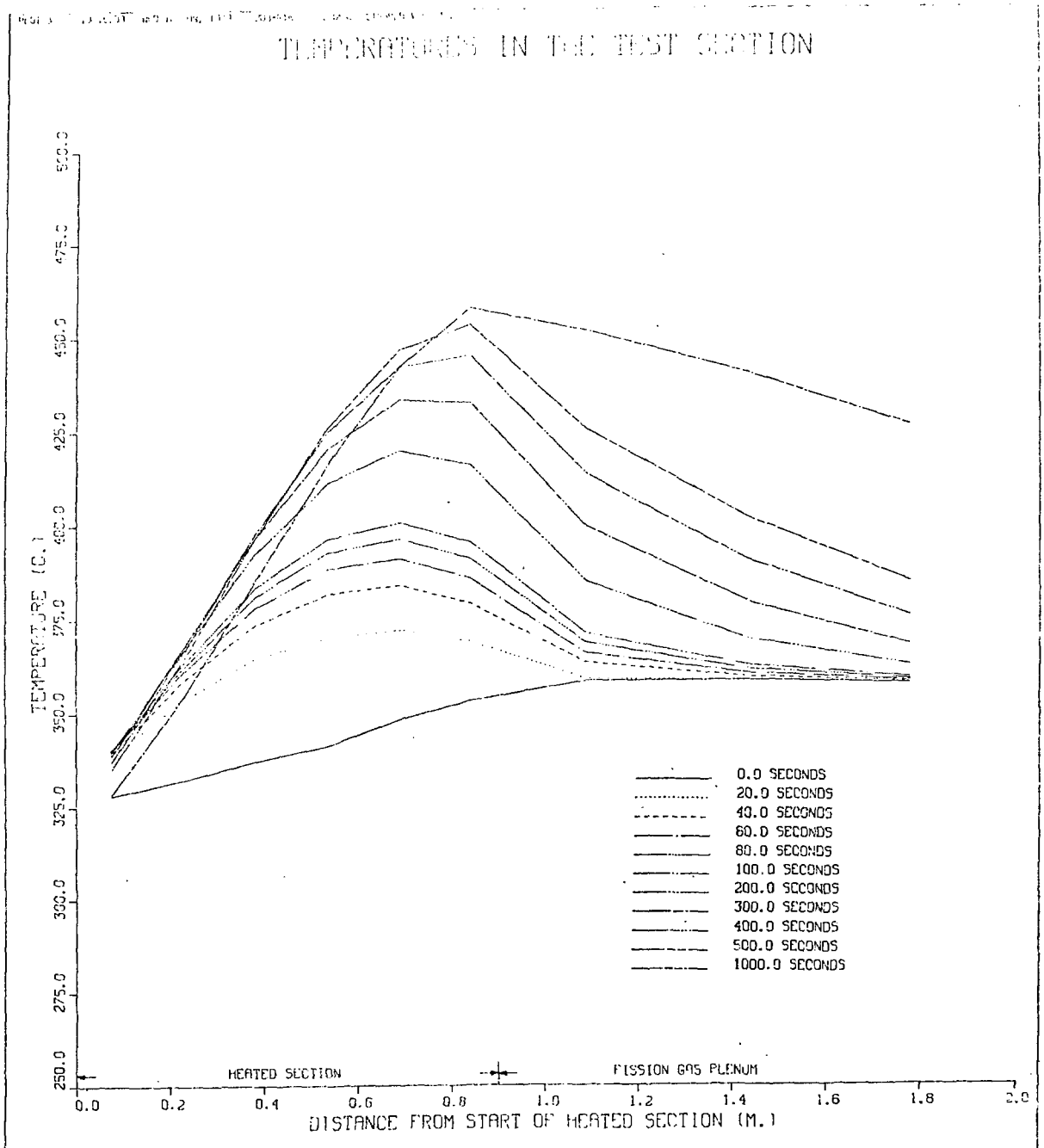

Figure 12A. Computed test section temperatures for various times early in the transient. LONAC simulation of THORS Bundle 6A, Test 39 (parallel assembly test).

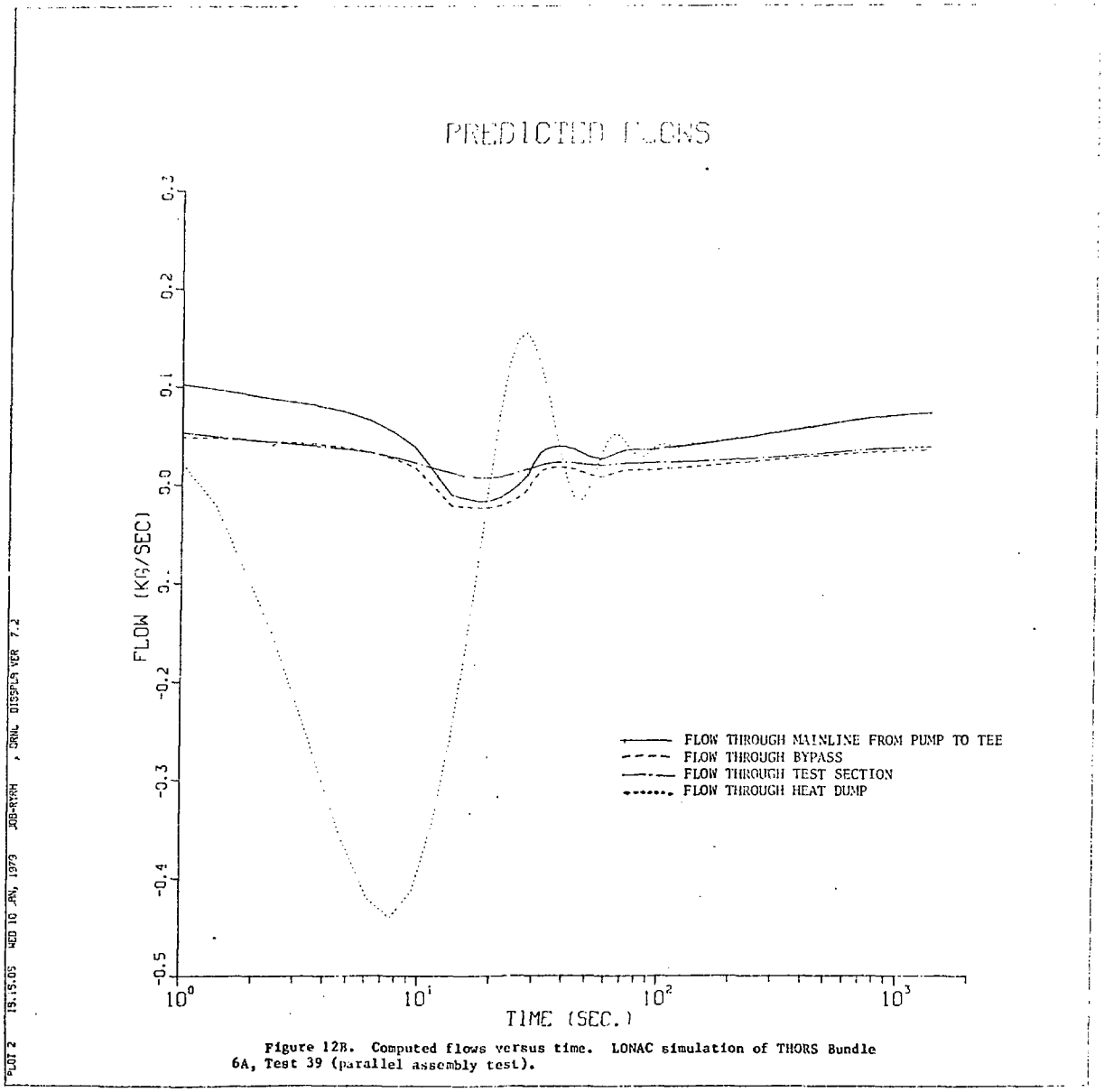

Figure 12B. Computed flows versus time. LONAC simulation of THORS Bundle 6A, Test 39 (parallel assembly test).